AN ASSESSMENT OF MECHANICAL BEHAVIOR OF FIBROUS POLYMERIC COMPOSITES UNDER DIFFERENT LOADING SPEEDS AT ABOVE- AND SUB-AMBIENT TEMPERATURES

A THESIS SUBMITTED IN PARTIAL FULFILLMENT OF THE REQUIREMENT FOR THE DEGREE OF

Master of Technology
in
Metallurgical and Materials Engineering
By

Renu Prava Dalai
Rollno.208MM109

Department of Metallurgical and Materials Engineering
National Institute of Technology
Rourkela-769008
2010

AN ASSESSMENT OF MECHANICAL BEHAVIOR OF FIBROUS POLYMERIC COMPOSITES UNDER DIFFERENT LOADING SPEEDS AT ABOVE- AND SUB-AMBIENT TEMPERATURES

A THESIS SUBMITTED IN PARTIAL FULFILLMENT OF THE REQUIREMENT FOR THE DEGREE OF

Master of Technology
in
Metallurgical and Materials Engineering

Under the Supervision of

Prof. B. C. Ray **Prof. B. B. Verma**

Department of Metallurgical and Materials Engineering
National Institute of Technology
Rourkela-769008
2010

National Institute of Technology
Rourkela

CERTIFICATE

This is to certify that the thesis entitled, " **An Assessment of Mechanical Behavior of Fibrous Polymeric Composites Under Different Loading Speeds at Above- and Sub - Ambient Temperatures** " submitted by Mrs. Renu Prava Dalai in partial fulfillment of the requirements for the award of Master of Technology Degree in Metallurgical and Materials Engineering at the National Institute of Technology, Rourkela (Deemed University) is an authentic work carried out by her under my supervision and guidance. To the best of my knowledge, the matter embodied in the thesis has not been submitted to any other University/Institute for the award of any Degree or Diploma.

Date:

Prof. B. C. Ray
Dept. of Metallurgical and Materials Engg.
National Institute of Technology
Rourkela-769008

Prof. B. B. Verma
Dept. of Metallurgical and Materials Engg.
National Institute of Technology
Rourkela-769008

.

Acknowledgement

I avail this opportunity to express my heartfelt gratitude and regards to **Prof. B. C. Ray**, Department of Metallurgical & Materials Engineering, National Institute of Technology, Rourkela for his invaluable guidance, untiring efforts and meticulous attention at all stages during my project work. An erudite professor and a strict disciplinarian, I consider myself fortunate to have worked under his supervision.

I would also like to convey my deep regards to my co-supervisor **Prof. B.B.Verma, HOD** Metallurgical and Materials engineering Department, for his indebted help and valuable suggestions for the accomplishment of my dissertation work.

My sincere regards to **Prof. A. Mallik**, Metallurgical and Materials Engineering Department, for her co-operation during the period of work.

I am also grateful to **Prof. A. Basu,** M. Tech. coordinator, for his valuable suggestion to bring out this thesis in time.

I am also thankful to **Mr. R. Patnaik, Mr. Sameer Pradhan and Mr. S. Hembram** Metallurgical & Materials Engineering, Technical assistants, for their help during the execution of experiment.

Special thanks to my family members, without their blessings and support, I could not have landed with this outcome.

RENU PRAVA DALAI

TABLE OF CONTENTS

PAGE NO.

Chapter 3

LIST OF FIGURES

Chapter 4

LIST OF TABLES

Abstract

Advanced fibrous polymeric composites are one of the most successful composite material systems due to its wide range of advantages such as high specific strength and stiffness, fatigue properties and corrosion resistance. Composite structures undergo different loading conditions i.e. from static to dynamic during their service life. During a cruise cycle an aircraft structure undergo different temperatures starting from ambient temperature on ground to during flight at 30,000 ft (-50˚C) and +50˚C during stays at the tropic and arid places. The polymer matrix is more susceptible to these changes than the fiber and thus dominates the mechanical behavior of FRP composites. Polymers are characterized as visco-elastic materials that their mechanical properties are strain rate dependent or they are called as sensitive to the rate at which loaded. The present experimental investigation uses flexural test to assess the effects of thermal conditioning at above- (50˚C) and below- (-50˚C) ambient temperature for multilayered laminates of 60 weight percentages of silane treated E-Glass fiber/epoxy composites and also with PAN based high strength epoxy compatible carbon fiber/epoxy composites. The state of interaction between the fiber and matrix was reflected in the ILSS values measured by 3 point-bend test with an Instron tensile testing machine with five increasing crosshead speed ranging from 1, 10,100,200 and 500 mm/min. Thermal conditioning at +50˚C is to induct further polymerization process in terms of epoxy embrittlement and along with the development of penetrating and/or semi penetrating network at the fiber/matrix interface. Whereas at −50˚C, the polymer chains get frozen due to which the deformation process is reduced results in less polymer relaxation i.e. it gets hardened. At higher crosshead speed due to shorter load assisted relaxation time, there is reduction in ILSS. The polymer gets more time for relaxation at lower crosshead speeds; as a result there is enhancement of ILSS values. The failure mechanisms are changing with changing in loading rate from static to dynamic. Fracture processes at the crack tip are controlled by thermal relaxation time and mechanical relaxation. At higher strain rates the heat generation was much faster than heat removal due to quasi-adiabatic heating which increases the fracture strain. In both the systems the locus of failure will shift from fiber polymer interface to the matrix itself that means instead of adhesion failure the predominating failure may be cohesive failure and that too shear cusp formation. FTIR analysis depicts that the band at 2609 cm^{-1} in the spectrum of

carbon/epoxy composite can't be seen properly in the spectra of the glass/epoxy systems. Carbon fiber may react with the OH groups which supports that the ILSS values are higher for CFRP than GFRP. DSC analysis shows an increase in glass transition temperature (T_g) after thermal conditioning for glass/epoxy composites. But for carbon /epoxy systems due to strong adhesion between the fiber and matrix T_g value is more as compared to glass/epoxy systems. But with increase in thermal conditioning time the T_g decreases due to the breakage of secondary bonds. AFM surface topography reveals that fiber/matrix height difference gradually increased with the increase of thermal treatment time at 50˚C for 5 hours suggested that residual stresses are developed due to this shrinkage. Implication of thermal conditioning most often lead an improved adhesion of the interface (at above ambient) and/ or increased crack density (at below ambient) temperature. These changes might lead further complications in accessing the loading rate sensitivity which itself as contradictory as on today.

Key words: Loading rate sensitivity, Thermal conditioning, ILSS, T_g, Post curing

CHAPTER 1

INTRODUCTION

Back ground of fibrous polymeric composites

Objective of the present work

Chapter 1

1. Introduction

1.1 Background of Fibrous Polymeric Composites:

History of human civilization evolved from the Stone Age where metals played a marginal role in engineering. The concept of fibrous polymeric composite started since 2000 B.C, in that era where engineering was dominated by polymers (wood, straw) and composites (like straw bricks). The true age of plastics was emerged just after 1900's with chemists and industrialists. They were taking bold steps to have the plastics desirable properties i.e. ease of formability, very low density compared with metals, excellent surface finish and corrosion resistance but lacked in stiffness. The first known FRP product was a boat hull manufactured in the mid 1930's as part of a manufacturing experiment using a fiberglass fabric and polyester resin laid in a foam mold. From this somewhat inauspicious beginning of FRP composites, applications have revolutionized entire industries, including aerospace, marine, electrical, corrosion-resistance and automotive and transportation. The same technology that produced the reinforced plastic hoops required for the Manhattan nuclear project in World War II, spawned the development of high performance composite materials for solid rocket motor cases and tanks in 1960's and 70's. In fact, fiberglass wall tanks were used on the Skylab orbiting laboratory to provide oxygen for the astronauts. In the 1960's, the British and U.S. Navies were simultaneously developing minesweeper ships as FRP composites are not only superior to other materials in a harsh marine environment, they are also non-magnetic in nature. That time it was also noticed that FRP's ability to reduce the radar signature of the structure, such as a ship or an aircraft. High performance of these composite materials has been demonstrated in advanced technology aircraft such as the F-117 Stealth Fighter and B-2 Bomber. Currently, FRP composites are being used for space applications and are involved in several NASA test initiatives. One very big concomitant advanced contemporaneous with the development of composite materials has been that of optical fiber communication [1]. FRP composites have been used as a construction material for several decades. During the late 1970's and early 1980's, many applications of composite reinforcing products were demonstrated in Europe and Asia. In 1986, the world's first highway bridge using

composites reinforcing tendons was built in Germany. The first composite bridge deck was demonstrated in China. The first all composites pedestrian bridge was installed in 1992 in Aberfeldy, Scotland. In the U.S., the first FRP reinforced concrete bridge deck was built in 1996 at McKinleyville, WV followed by the first all-composite vehicular bridge deck in Russell. What is undoubtedly true is that the high performance components used in advanced composites represents a larger fraction of the overall value of the composite market [2].

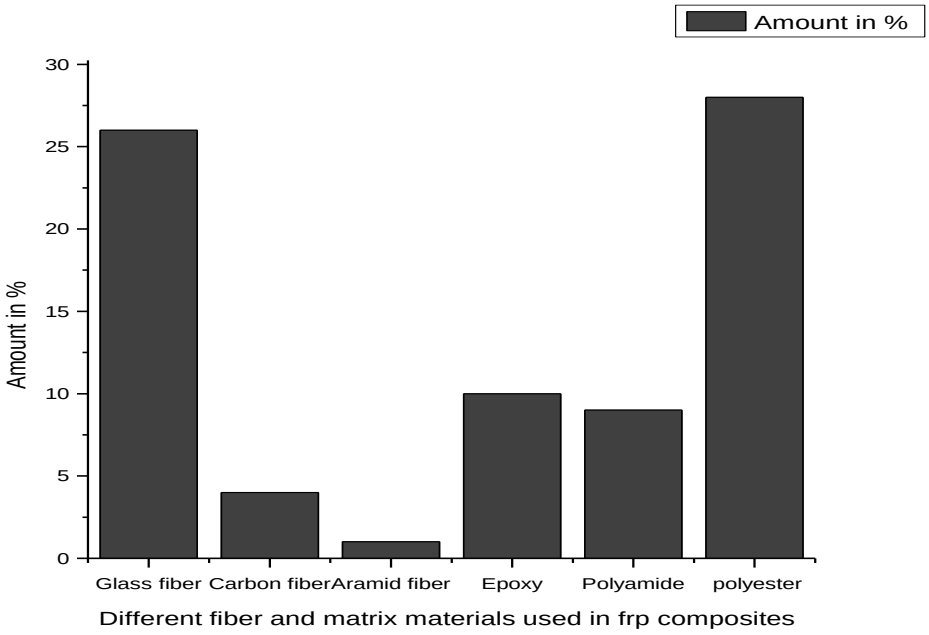

Fig.1.1 Percentages of the overall value of the fiber reinforce composite market of fibers and matrix materials

Challenges

It has been shown that FRP composites have the potential to revolutionize the construction of buildings, producing dramatic new forms and in some cases more efficient and cost effective structures. It is expected that this will initially be in niche areas, but could also penetrate mass markets such as housing construction. The adoption and efficient use of FRP materials will be a challenge to traditional architects and engineers. For the 21st century, composite fabricators and suppliers are actively developing products for the civil infrastructure, considered to be the largest potential market for FRP composites. Concrete repair and reinforcement, bridge deck repair and

new installation, composite-hybrid technology (the marriage of composites with concrete, wood and steel), marine piling and pier upgrade programs are the some of the areas that are currently being explored. Selection of the optimal reinforcement and material is dependent on the property requirements of the finished part.

Table 1.1 Applications of FRP composite materials

Industry	Examples	Comments
Aircraft	**Doors, elevators, rubbers, landing gears, fuselage, tail spoiler, body etc.**	Usually result in 20 to 30% weight savings over metal parts
Aerospace	**Space shuttle, space station**	Great weight savings, Dimensional stability and low CTE
Automotive	**Body frame, chassis components, engine components, drive shaft, exterior body components, leaf springs**	High stiffness and damage tolerance, good surface finish, lower weight and higher fuel efficiency
Marine	**Hulls and masts for recreational boats, submersibles, spars, decks and bulkheads**	Weight reduction results in higher boat cruising speed and distance, fast acceleration
Sporting goods	**Tennis and racquetball racquets, golf club shafts and heads, bicycle frames, helmets, race cars etc.**	Weight reduction, Vibration damping, Design flexibility
Chemical, Construction and Electrical	**Pipes, tanks, pressure vessels, structural and decorative panes, bridges, housings, printed circuit boards, insulators, computer housing**	Weight savings, corrosion resistance, portable, high specific properties
Railway	**Window frames & shutters, wall protector in toilets, chain cover for jmp jack, air grill for ac coach, axle box covers**	Weight savings, lower thermal expansion properties, high specific strength properties and corrosion resistance

Composite materials offer several advantages over conventional materials such as high specific strength, specific stiffness, fatigue and impact resistance and corrosion resistance.

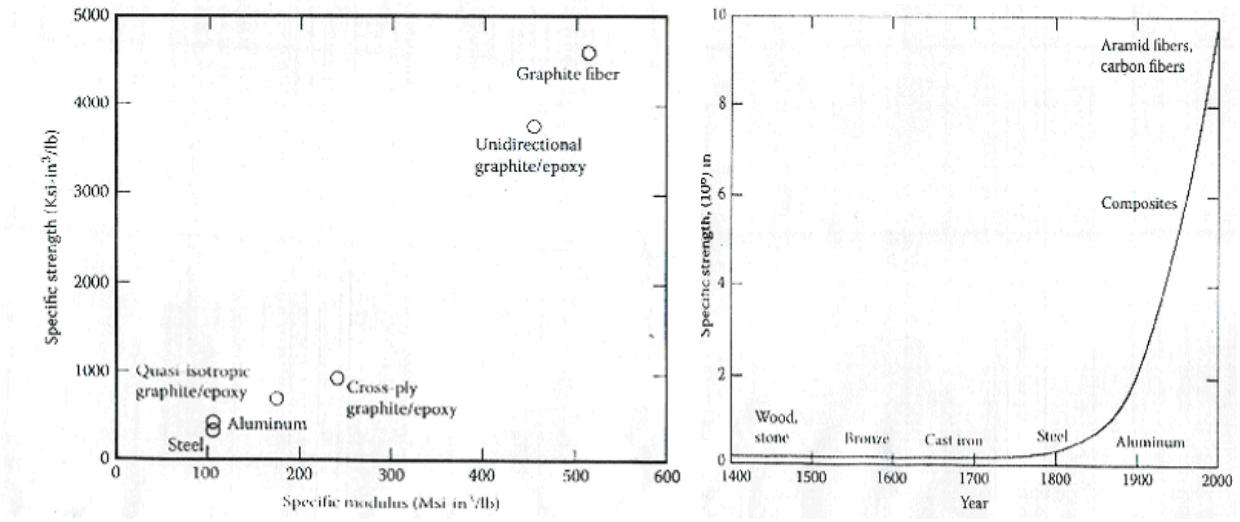

Fig.1.2 Specific strength versus specific modulus and Year [3]

Composites are superior to metals in specific strength and stiffness. Weight reduction is a key consideration for automotive industries and aerospace for better fuel efficiency. Coefficients of thermal expansion are for many fiber composites are much lower than those of metals. Due to this composite structures may exhibit better dimensional stability if a variation in service temperature is occurred. Because of heterogeneous nature of these composites provides several energy- dissipation mechanisms on a microscopic scale comparable to the yielding process such as fiber pull-out, interfacial de-bonding, matrix cracking and fiber fracture. The mechanical behavior of composites depends on the individual constituent i.e. the fiber and matrix properties and also on the fiber/matrix interface. Because of the presence of the two different constituents (fiber and matrix) and the fiber/matrix interface several complicating factors arises. The fiber/matrix interfacial bond greatly influences the mechanical behavior of composite materials because it transmitting the load from the matrix to the fibers. The fiber/matrix interface mechanical properties are also sensitive to the loading rate. The failure mode in the GFRP laminates changes from fiber brittle failure with fiber pullout at quasi-static crosshead rates, to brittle failure with considerable matrix damage as the cross head speed increases. E-Glass fibers have been found to be rate sensitive, information available in literature was not extensive to draw

any concrete conclusion. Woven and unidirectional GFRP are rate dependent, both the modulus and strength increase as the test rate are increased, strain to failure decrease with increasing strain rate. There is lack of rate dependency in carbon fiber reinforced plastics (CFRP). At quasi-static strain rate, micro and macro level defects in the materials play a major role to initiate and propagate the damage utilizing most of the applied energy. The mechanical properties of FRP composites are affected by different temperatures, due to this there is a dramatic change in the material. As because of there is a dearth of published information on these i.e. effects of loading rate at different temperature that necessitate the need for a more critical understanding of durability and sustainability of mechanical performances we are interested to work on this area.

1.2 Objective of the present project work

1. Assessment of mechanical behavior of glass- and carbon- fiber reinforced epoxy matrix composites:

1. Effect of changing loading rate at above- and sub- ambient temperature by flexural (Short Beam Shear) testing technique
2. Failure mechanism study of the thermal conditioned samples after Short Beam Shear test by SEM micrographs
3. Effect of thermal conditioning on the glass transition temperature of glass/epoxy and carbon/epoxy systems
4. Characterization of small interaction between the fibers and matrix by FTIR-imaging techniques.
5. Characterize the effect of thermal conditioning on surface topography of the composite systems by AFM

2. Effects of Temperature and Loading Speed on Inter-laminar Strength of FRP Composites:

1. Effect of thermal conditioning on the ILSS values at above- the glass transition temperature and at above- and below- ambient temperature of glass/epoxy composites by Short Beam Shear test.

2. Failure mechanism of the tested samples by SEM micrographs

CHAPTER 2

LITERATURE SURVEY

PREAMBLE

FIBER REINFORCED COMPOSITES

TYPES OF FIBER USED IN FRP COMPOSITES

MATRIX MATERIALS

INTERFACES AND INTERPHASES IN COMPOSITES

EFFECTS OF LOADING RATE ON FRP COMPOSITES

FAILURE MODES AT DIFFERENT STRAIN RATES

ENVIRONMENTAL IMPLICATIONS

Chapter 2

2. Literature Review

2.1 Preamble

This chapter introduces the common types of fibers and matrix material such as epoxy, their structures, and properties. The literature survey is based on the broad topic of interest i.e. the effect of loading rate and temperature on advanced fibrous polymeric composites.

2.2 Fiber Reinforced Polymer (FRP) Composites:

Advanced fibrous polymeric composites technologically the most important composites, consists of high strength and high modulus fibers embedded in or bonded to a low modulus matrix. The fiber utilizes the visco-elastic displacement of the low modulus matrix under stress to transfer the load to the fiber. It results a high strength and high modulus composite.

2.3 Fiber reinforcement

The three main fibers used in the construction industry are glass, carbon and aramid fibers. The most suitable of these fibers for a particular structural application depends primarily upon the required strength, stiffness, corrosion resistance.

2.3.1Glass fiber:

Glass fibers are silica based glass compounds that contain several metal oxides which can be tailored to create different types of glass. The main oxide is silica in the form of silica sand, the other oxides such as Ca, Na and Al are incorporated to reduce melting temperature and impede crystallization. The most important grades of glass are:

E-glass: E glass has low alkali content of the order of 2%. It is used for general purpose structural applications and it is used in construction industry, it has good heat and electrical resistance.

S-glass: It is a stronger and stiffer fiber with a greater corrosion resistance than the E-glass fiber. It has good heat resistance capacity.

C-glass: C glass has good corrosion resistance to acid and bases and has chemical stability in chemically corrosive environments**.**

R-glass: R glass has a higher tensile strength and tensile modulus and greater resistance to fatigue, aging and temperature corrosion to that of E glass.

Table.1.1Compositions of different types of glass used for fiber manufacture [4]

Constituents	E-glass	C-glass	S-glass
SiO2	**55.2**	**65**	**65**
Al2O3	**14.8**	**4**	**25**
B2O3	**7.3**	**5**	**-**
MgO	**3.3**	**3**	**10**
CaO	**18.7**	**14**	**-**
Na2O	**0.3**	**8.5**	**-**
K2O	0.2	-	-

2.3.1.1Structure of glass fiber

The polyhedron network structure of sodium silicate glass is shown in fig.1. Each polyhedron is a combination of oxygen atoms around a silicon atom bonded together by covalent bonds. The sodium ions form ionic bonds with charged oxygen atoms and are not linked directly to the network. The three dimensional network structure of glass fiber results isotropic properties with strong covalent bonding between atoms, which results in a high strength in three dimensions.

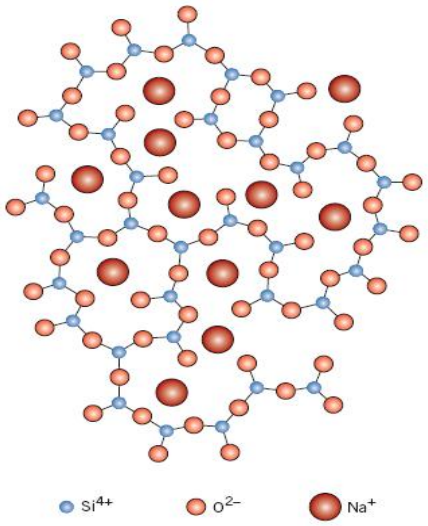

Fig.2.1 schematic representation of ion positions in a sodium–silicate glass [5].

2.3.1.2 Surface treatment of fibers

Surface treatment is done to improve the adhesion of fillers and fibers to matrix resin by modifying the surface of the solid. Often, chemical structure and sometimes topology of the surface change upon the treatment.

2.3.1.3 Silane treatments of glass fibers

Sizing materials are coated on the surface of the glass fibers as protection against mechanical damage. For glass reinforcement the sizing usually contains a coupling agent to bridge the fiber surface with the resin matrix used in composite. These coupling agents are usually organosilanes with the structure X3SiR.The R group may able to react with a group in the polymer matrix, the X groups can hydrolyze in the presence of water to form silanol groups which can condense with the silanol groups on the surface to the glass fibers to form siloxanes. The subject of silane chemistry and its interaction with both glass surface and polymer resins have been studied extensively, the silane coupling agent improving the bond quality between the fiber and matrix. In addition to the adhesion promotion, coupling agents aid in protecting fiber surfaces and prevent inhibition of polymerization by the solid surfaces. A small amount of a coupling agent can often dramatically improve the mechanical and physical properties of composites. The chemical reaction of a coupling agent occurring during the treatment and drying of the filler is shown below using a silane coupling agent [6].

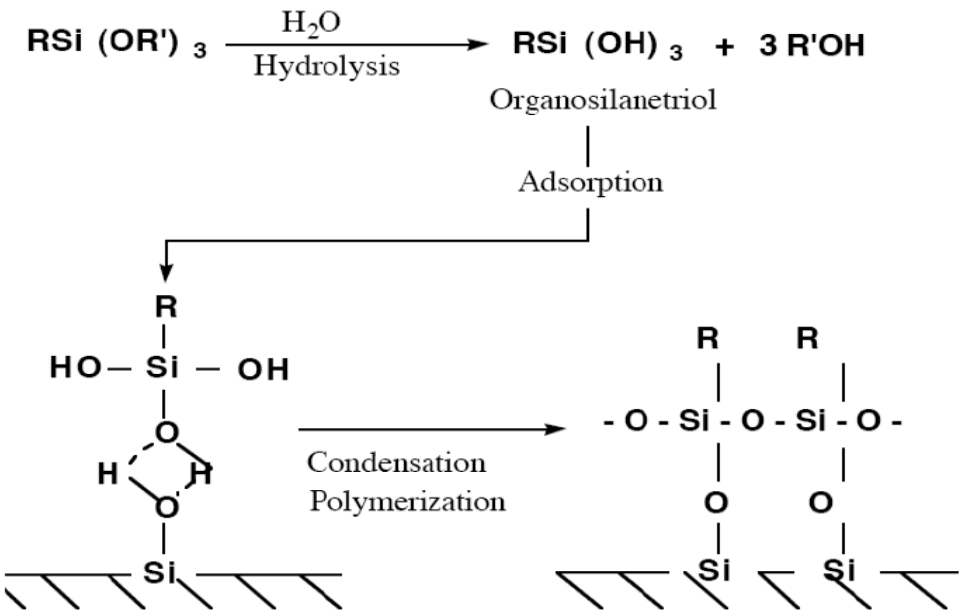

Fig.2.2 chemical process during surface treatment silaceous material by a silane coupling agent

2.3.2 Carbon fiber

Carbon fibers are about 0.005–0.010 mm in diameter and composed mostly of carbon atoms. The carbon atoms are bonded together in microscopic crystals that are more or less aligned parallel to the long axis of the fiber. The crystal alignment makes the fiber very strong for its size. Several thousand carbon fibers are twisted together to form a yarn, which may be used by itself or woven into a fabric. The density of carbon fiber is also considerably lower than the density of steel, making it ideal for applications requiring low weight. There are three types of precursors used currently to manufacture carbon fiber. Carbon fibers made from PAN precursors have higher tensile strengths than other precursor based fibers.

2.3.2.1 Structure of carbon fiber

In a graphite single crystal the carbon atoms in a basal plane are arranged in hexagonal arrays and held together by strong covalent bonds. Between the basal planes only weak van der Waal forces exist. Carbon fibers can be classified depending on the precursor used, the most commonly used precursors are rayon based fibers, polyacrylonitrile (PAN) and pitch.

Fig.2.3 schematic view of a three-dimensional model of a carbon fiber [7]

Table2.3 Typical properties of different types of Carbon Fiber

Properties	Density	Young's modulus	Tensile strength	Tensile elongation
High strength	1.8	230	2.48	1.1
High modulus	1.9	370	1.79	0.5
Ultra-high modulus	2.0-2.1	520-620	1.03-1.31	0.2

2.3.3 Kevlar fiber (Aramid)

Kevlar brand fiber is an innovative technology from DuPont that combines high strength with light weight to help dramatically improve the performance of a variety of consumer and industrial products. Light weight and flexible, Kevlar has evolved over four decades of innovation to do everything from helping save thousand of lives around the world to helping make safer homes and vehicles to helping land spacecraft on Mars.

2.3.3.1Structure of Kevlar fiber

The rigid linear molecular chains are highly oriented in the fiber axis direction, with the chains held together in the transverse direction by hydrogen bonds. The strong covalent bonds in the fiber axis direction provide high longitudinal strength, where as the weak hydrogen bonds in the transverse direction result in low transverse strength.

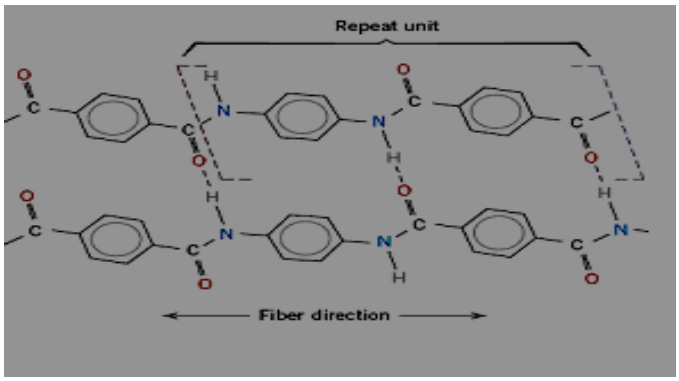

Fig.2.4 Schematic representation of repeat unit and chain structures for Kevlar fiber

2.3.3.2 Types of Kevlar fiber:

Today, there are three grades of Kevlar available: Kevlar 29, Kevlar 49, and Kevlar 149. The table below shows the differences in material properties among the different grades

Table 2.3 properties of different grades of kevlar fiber

Density g/cm	Grade	Tensile Modulus (GPa)	Tensile Strength (GPa)	Tensile Elongation in %
1.44	29	83	3.6	4.0
1.44	49	131	3.6-4.1	2.8
1.47	149	186	3.4	2.0

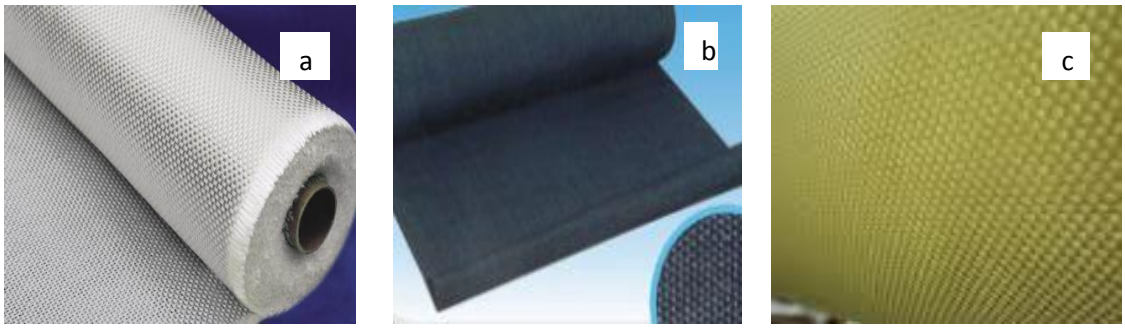

Fig.2.5 woven roving glass (a), carbon (b) and Kevlar (c) fabrics

Table 1.2 Properties of continuous and aligned glass-, carbon-, and aramid-fiber reinforced epoxy-matrix composites in longitudinal and transverse directions. in all cases the fiber volume fraction is 0.60[5]

Property	E-glass	Carbon(high strength)	Aramid(Kevlar 49)
Specific gravity	**2.1**	**1.6**	**1.4**
Tensile modulus			
Longitudinal(GPa)	**45**	**145**	**1380**
Transverse	**12**	**10**	**30**
Tensile strength			
Longitudinal (MPa)	**1020**	**1240**	**1380**
Transeverse (MPa)	**40**	**41**	**30**
Ultimat tensile strain			
Longitudinal	**2.3**	**0.9**	**1.8**
Transeverse	**0.4**	**0.4**	**0.5**

2.4 MATRIX MATERIALS

A polymer (matrix) is an organic material composed of molecules made from many repeats of the same monomer. Thermosetting polymers are usually made from liquid or semi solid precursors which harden irreversibly. The chemical reaction is known as polymerization or curing and on completion the liquid resin is converted to a hard solid by chemical cross linking which produces three dimensional networks of polymer chains. The main polymers used in this category are the epoxies, vinyl ester, unsaturated polyester and the phenolics.

2.4.1Functions of the matrix material

- wet out the fiber and cure satisfactorily during manufacturing
- bind together the fibers and to protect their surfaces from abrasion and corrosion due to different environment
- disperse the fibers and to separate them to avoid any catastrophic propagation of cracks
- transfer stresses to the fibers efficiently by adhesion and/or friction and to reduce the chances of failure in the matrix
- chemically and thermally compatible with the fibers over long periods of time

There are several different types of polymer matrices can be used in advanced fibrous composites. The two types of polymer which can be used in FRP composites are thermosetting and thermoplastic polymers. Thermoplastic polymers are long chain molecules held together by relatively weak Van der Walls forces, they derive their strength and stiffness from the inherent properties of the monomer units and very high molecular weight.

2.4.2 EPOXY RESIN

Epoxy resins are the most common material for high performance advanced fibrous polymeric composites, but they are inherently brittle because of their high degree of cross linking. The densely cross linked structure are the basis of superior mechanical properties such as high modulus, high fracture strength, solvent resistance. However these materials are irreversibly damaged by high stress due to the formation and propagation of cracks. The most important epoxy resins are characterized by the existence of the epoxy group, which is a three member ring with ring with two carbons and an oxygen atom.

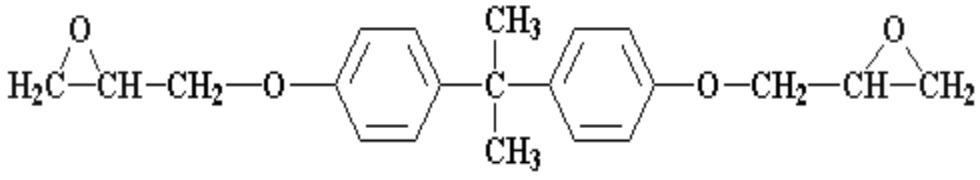

Fig.2.6 epoxide groups and related reactants [4]

2.4.2.1 Curing of epoxy

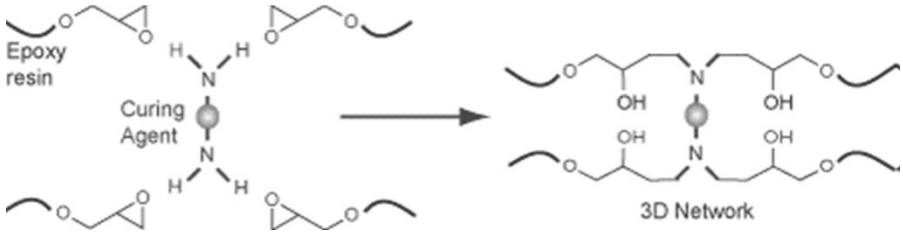

Fig.2.7 the curing of epoxy resin with primary amines [4]

2.5 Interfaces and Interphases in Composites:

The concept of controlled an engineered interface is given preference because it is likely to affect the overall mechanical behavior of fiber-reinforced composites. The structural integrity and lifetime of fibrous polymeric composites are critically depends on the stability of the fibers and the fiber/matrix interface region.

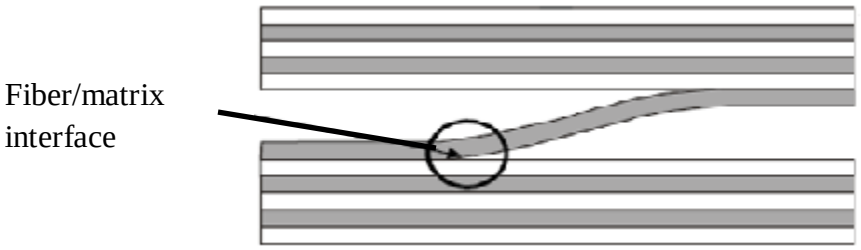

Fig. 2 .8 Interface between the fiber and matrix [8]

The mechanical behavior of composites not only depends on the constituent fiber and matrix properties but also on the fiber/matrix interface. The interface is responsible for transmitting the load from the matrix to the fibers, which contribute the greater portion of the composite strength. In contrast interphase is a two dimensional mathematical plane having some finite unknown thickness [9], wherein the chemical, physical and mechanical properties vary either continuously or in a stepwise manner between those of the bulk fiber and the matrix materials[10]. Better the interfacial bond better will be the ILSS, de-lamination resistance, fatigue and corrosion resistance [4]. The interactions between the fiber and matrix resin during thermal treatment are complex but important phenomena. These interactions may often lead to the formation of inter-phase.

2.6 EFFECTS OF LOADING RATE ON FRP COMPOSITES

The present review report emphasizes on the loading rate sensitivity of fiber reinforced polymeric composites, as the past researches in this area is bit far from any concrete conclusion. Testing on bulk composite materials has a more serious limitation than in micro-composite tests in that the actual locus and modes of failure have to be consistent with what are originally designed for the composite in order for a specific task is to be valid [10]. Fibrous polymeric composites armed with a wide range of advantages, it play major role in various sectors such as aerospace, transportation, chemical industry, electrical and electronic parts, construction, consumer and sports good. Composite structures undergo different loading conditions during their service life, e.g. sports equipment at high loading rate to pressure vessels at low loading rates [11]. The effects of varying loading rates on mechanical properties of FRP composites are investigated and observed a variety of contradictory observations and conclusions [12]. The fiber/matrix interfacial bond greatly influences the mechanical behavior of composite materials because it transmitting the load from the matrix to the fibers [13]. The fiber/matrix interface mechanical properties are also sensitive to the loading rate. The de-bonding forces, frictional sliding forces and apparent shear strength values increase with increasing displacement rate [14]. From the past researches the data describing that influence of strain rate on the mechanical properties are sparse the studied composite materials are glass/epoxy and carbon/epoxy [15]. The failure mode in the GFRP laminates changes from fiber brittle failure with fiber pullout at quasi-static crosshead rates, to brittle failure with considerable matrix damage as the cross head speed increases [16]. E-Glass fibers have been found to be rate sensitive, information available in literature was not extensive to draw any concrete conclusion. Woven and unidirectional GFRP are rate dependent, both the modulus and strength increase as the test rate are increased, strain to failure decrease with increasing strain rate [17-19]. Thermal degradation of epoxy resin involves chemical reaction and physical changes. Chemical reaction is represented by oxidation, further cross-linking and further reaction of un-reacted monomers, while physical change is the visco-elastic behavior [20]. The visco-elastic yield behavior of polymer is generally temperature and loading rate dependent [21]. The thermal conditioning results in post-curing strengthening effect [22]. The present investigation has been focused on the loading rate and temperature dependence of glass/epoxy composites. There is a dearth of published information on these areas that

necessitate the need for a more critical understanding of durability and sustainability of mechanical performances.

Matrix resins such as polyester and epoxy are known to be highly rate sensitive, both the initial modulus and maximum strength increases with increasing strain rate. Glass fiber reinforced plastics (GFRP) have been found to be rate sensitive, a direct correlation between the rate dependency of the composite and those of the constituent phases can be difficult. The lack of a significant rate dependency of carbon fiber reinforced plastics (CFRP) likely reflects the lack of rate dependence of the carbon fiber [4]. At quasi-static strain rate, micro and macro level defects in the materials play a major role to initiate and propagate the damage utilizing most of the applied energy. At higher strain rates, the polymer not gets enough time to realize the material internal defects during loading [23]. Different fracture processes occur at the crack tip at different strain rates and the fracture processes are controlled by two scales of time mechanical relaxation time and thermal relaxation time. At Low strain rate (loading time>mechanical relaxation time) here small isothermal, plastic deformations occur at the crack tip, increase the crack resistance and make the fracture strain higher. Medium strain rate (loading time< mechanical relaxation time) time is not sufficient for plastic deformations at the crack tip, polymer becomes more brittle and fracture strain is decreased. High strain rate (loading rate > thermal relaxation time) increased heat power generation at the crack tip by deformation and fracture, but most of the heat is removed by thermal conductivity. Very high strain rate (loading rate < thermal relaxation time) heat generation is faster than its removal, quasi-static adiabatic heating at the crack tip occurs which enhances plastic deformation and strain at yield increased [24]. Alignment of fibers makes the material more efficient in carrying the load, thus increasing the strength and enabling the material to approach its theoretical strength, as predicted by the rule of mixture, after short periods of pre-stress when tested to failure [25].

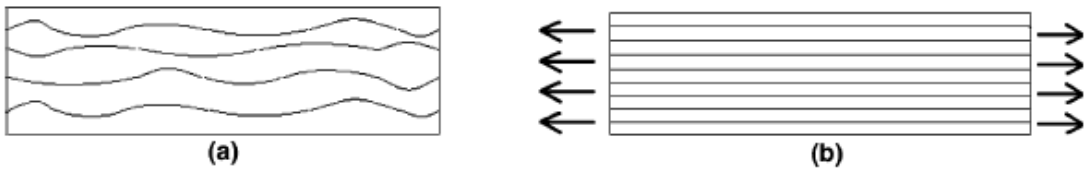

Fig. 2.9 Fiber alignments due to applied stress (a) before loading (b) after loading [8]

Fig.2.9 shows the material with the typical fiber misalignment during processing (a), and the composite material with the aligned fibers due to the applied stress (b).

2.6.1 Strain rate sensitivity

The rate at which strain is applied to a specimen can have an important influence on the flow stress. The crosshead speed velocity, $v = \frac{dL}{dt}$

Strain rate is expressed in terms of linear strain rate is ė

$$\dot{e} = \frac{de}{dt} = \frac{d(L - L_0)/L_0}{dt} = \frac{1}{L_0}\frac{dL}{dt} = \frac{v}{L_0} \quad (1)$$

Equation 1 indicates that for a constant crosshead speed the true strain rate will decrease as the specimen elongates [26].

The true strain rate is given by

$$\dot{\varepsilon} = \frac{d\varepsilon}{dt} = \frac{d[\ln(L/L_0)]}{dt} = \frac{1}{L}\frac{dL}{dt} = \frac{v}{L} \quad (2)$$

$$V = \dot{\varepsilon} L_0 \exp(\dot{\varepsilon} t) \quad (3)$$

The relationship between the flow stress σ and strain rate $\dot{\varepsilon}$, at constant strain and temperature is

$$\sigma = C(\dot{\varepsilon})^m \quad (4)$$

$$m = \left(\frac{\partial \ln \sigma}{\partial \ln \dot{\varepsilon}}\right)_{\varepsilon,T} = \frac{\dot{\varepsilon}}{\sigma}\left(\frac{\partial \sigma}{\partial \dot{\varepsilon}}\right)_{\varepsilon,T} = \frac{\Delta \log \sigma}{\Delta \log \dot{\varepsilon}} = \frac{\log \sigma_2 - \log \sigma_1}{\log \dot{\varepsilon}_2 - \log \dot{\varepsilon}_1} = \frac{\log(\sigma_2/\sigma_1)}{\log(\dot{\varepsilon}_2/\dot{\varepsilon}_1)}$$

Where m is known as the strain rate sensitivity, Strain rate sensitivity of metals is quite low (<0.1) at room temperature but m increases with temperature. When a unidirectional composite layer is heated from the initial temperature T_o to a final temperature T and is subjected to stresses σ_i, the resulting strains ε_i are obtained as the sum of the mechanical strains ε_i^{σ} and the thermal strains ε_i^{T} [27].

$$\varepsilon_i = \varepsilon_i^{\sigma} + \varepsilon_i^{T}$$

2.6.2 GLASS/EPOXY COMPOSITES

Glass fibers have loading rate dependent, tensile tests were performed on a RE200 glass/epoxy composite laminates at low strain rates from 0.0001 to 0.11S $^{-1}$ and reported that the mechanical behavior such as the longitudinal ultimate strength increased by 24.7% whereas the increase in longitudinal Young's modulus was 4.2% [16]. The effect of strain rate from 0.008 mm/s to 4 m/s was used to study the tensile properties of a woven glass (Tuflon)/epoxy composite and concluded that the tensile, shear and flexural energy increase in 17%, 5.9% and 8.5% respectively with increasing in log of strain rate [28]. The modulus, failure strength and failure modes are found to be rate sensitive, when the tests were performs on a dynamic testing technique over a range of 10^{-4} to 10^{3} S^{-1} on glass/epoxy and carbon epoxy composites.

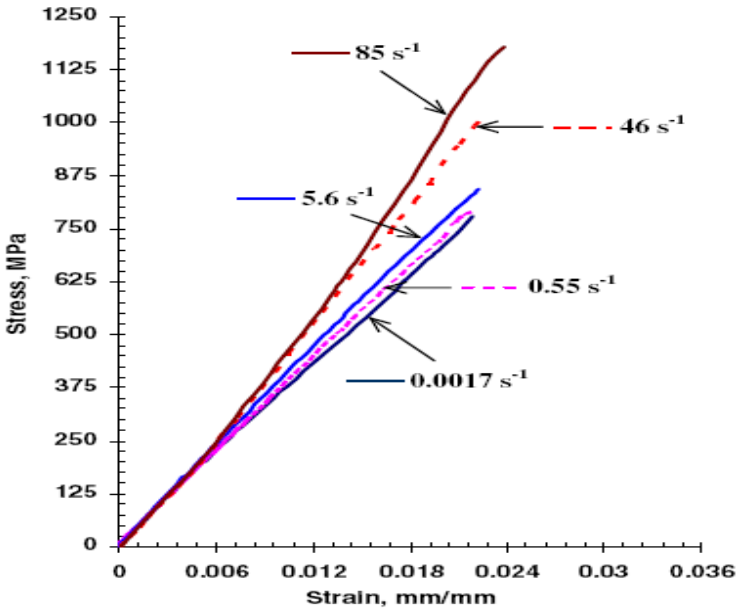

Fig. 2.10 Typical stress–strain tensile behavior of glass/epoxy composites under various strain rates [28].

It was explained that the increase in failure strength was due to change in failure modes with strain rate [17]. Tensile failure properties of unidirectional glass/epoxy composites were studied at various strain rates from 0.001 to 100 S^{-1} using a high-speed servo-hydraulic testing apparatus. The experimental results show an increase in tensile strength, modulus, strain to failure and absorbed failure energy of 52%, 12%, 10% and 53%, respectively [29]. Fig.2.10 shows a load rate dependency for glass/epoxy composites at different strain rate. Brittle thermo-set epoxy

resin can undergo a limited extent of deformation prior to failure [30]. The ductility of a matrix resin may become a limiting factor at a high strain rate for the composite, strength. It is more ductile than it's composite at a lower strain rate [31].

2.6.2 CARBON/EPOXY COMPOSITES

A small rate dependence of the strength has been observed with woven reinforced CFRP, where as unidirectional CFRP is relatively rate dependent when loaded in the fiber direction [4]. As the loading rate increase from quasi-static to dynamic the average value of the shear stress on the failure plane increases by about 70% for the carbon/carbon interfaces in carbon/epoxy composites in case of double-lap shear test[32].

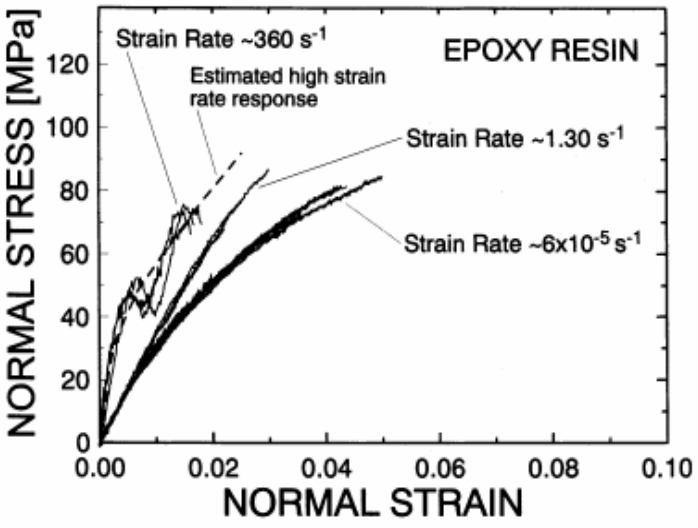

Fig. 2.11 Stress–strain curves for the epoxy resin at different strain rates [32].

Fig. 2.11 shows that the initial response at the low and moderate strain rate is linear and nearly the same, but in the nonlinear range, it follows that the deformation is stiffer in the moderate stain rate tests. The response at the high strain rate is stiffer than at the lower strain rates. The maximum stress increases somewhat with strain rate, but the increase is not significant [33]. Carbon/epoxy composites were tested at different strain rates of about $10^{-3}S^{-1}$ for quasi-static, 1 S^{-1} for intermediate rate and 10^{3} S^{-1} for dynamic tests, used for determining the inter-laminar shear properties of the material at low, intermediate and high strain rates.

2.7 Failure modes at different strain rates

Fiber reinforced polymer composites undergo different loading conditions during service and their failure modes are changing with changing in loading rates from static to dynamic loading conditions. The present experimental investigation is on the effect of loading rate on different failure modes of glass, carbon reinforced epoxy matrix composites.

The main causes of failure can be:

(a) Breaking of fibers

(b) Interfacial de-bonding

(c) Micro-cracking of the matrix

(d) Fiber pull-out

(e) Stress redistribution

(f) De-lamination.

In case of shear loading the decisive limiting parameter is the ILSS for composites. If this value is exceeded, de-lamination of composite layers occurs. Fiber breakage occurs at loads defined by bending strength. The ILSS measurements are performed in short beam tests. The values of ILSS are determined mainly by failures of the matrix, interfacial bond or fibers [34].

2.7.1 GLASS/EPOXY COMPOSITES

Facture of composites can occur in a cohesive or adhesive manner, adhesive failures are expected when the fiber/matrix interface is weak. Failure in a fiber composite may initiates from small defects such as broken fibers, matrix pores and de-bonded interfaces .The failure modes changes from fiber brittle failure with fiber pull out at quasi-static cross-head speeds to brittle failure with considerable matrix damage preceding final fracture as the cross-head rates increases from intermediate to high. At lower strain rates the GFRP material undergoes global failure where as at higher strain rates it is suggested that the polymer matrix undergoes localized failure depicted by the higher stiffness values. The main modes of failure for GFRP at high strain rates are de-lamination and de-bonding with very little fiber buckling, kinking or fiber breakage [18].

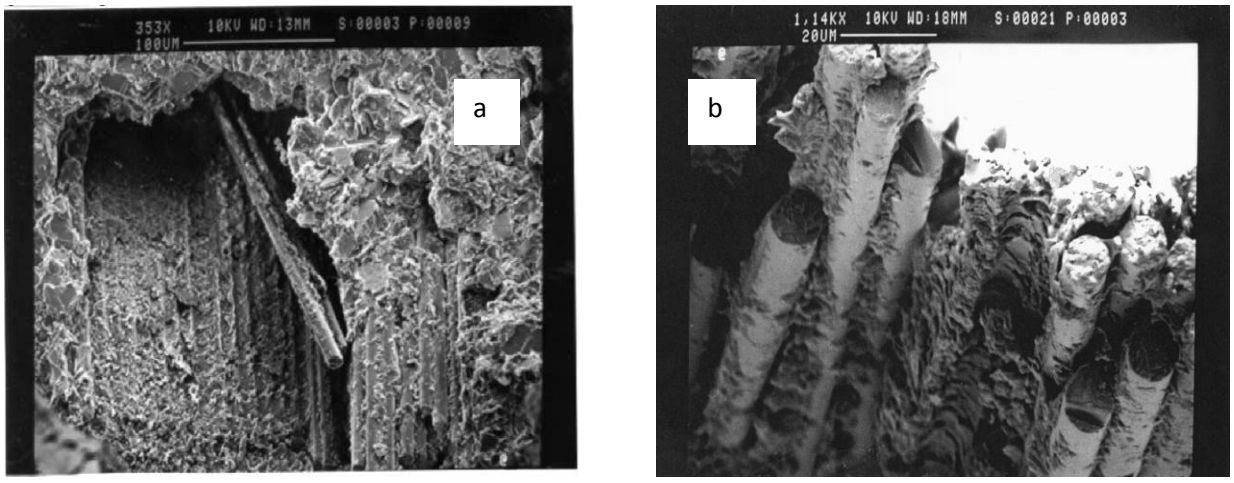

Fig. 2.12 Tufnol 10G/40 Laminate showing (a) fiber bunch pull-out with signs of fiber-matrix adhesion (b)exposed fibers indicating matrix de-lamination and de-bonding [14].

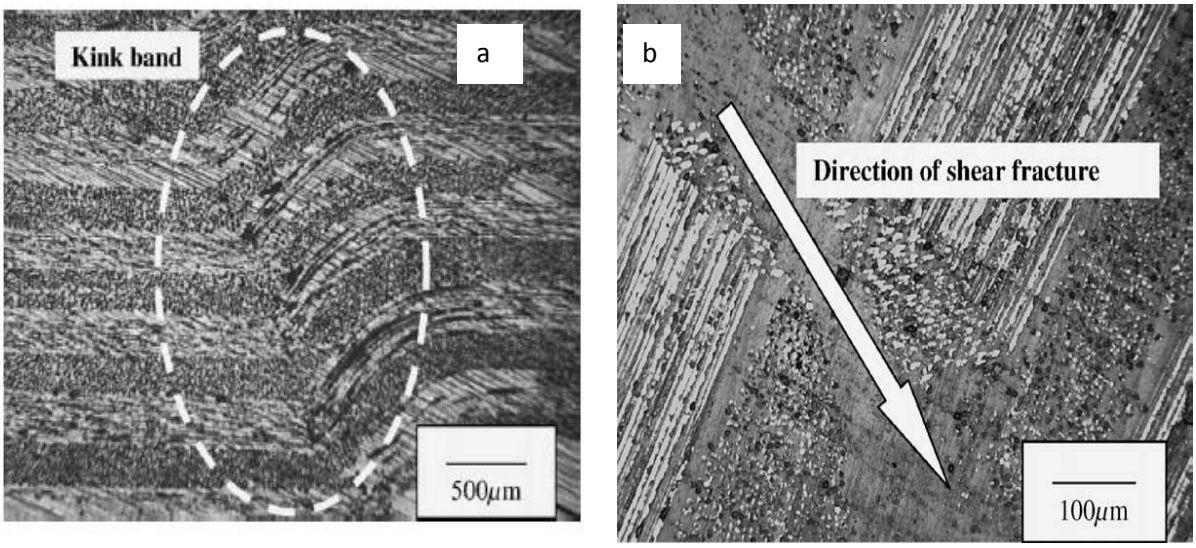

Fig.2.13(a) Shear fracture and kinking from quasi-statically loaded GFRP showing direction of shear fracture propagation and (b) Shear fracture from quasi-statically loaded CFRP showing direction of shear fracture propagation [18].

2.7.2 CARBON/EPOXY COMPOSITES

At low strain rates (quasi-static) the dominant damage mode for CFRP was shear failure, Fig. 8. Prevails this failure mechanism is typical for brittle materials. De-bonding occurs as a result of failure initiated at a point in the fiber/matrix interface which then propagates through the entire length of the interface. There was a greater density of resin debris and fiber fracture of the specimens tested at high strain rate [35]. Under tensile loading conditions, interplay failure

reveals a cleavage like appearance in the epoxy resin, when shear stress dominate the fracture process, the epoxy resin reveals a series of hackle markings on the fracture surface, which presumably reflect the coalescence of many tension induced micro-cracks inclined at an angle to the overall fracture plane[36]. For carbon/epoxy composites, where damage accumulation includes the formation of shear cusps involves plastic flow, the process is likely to show small strain rate dependence in single lap shear test [37].

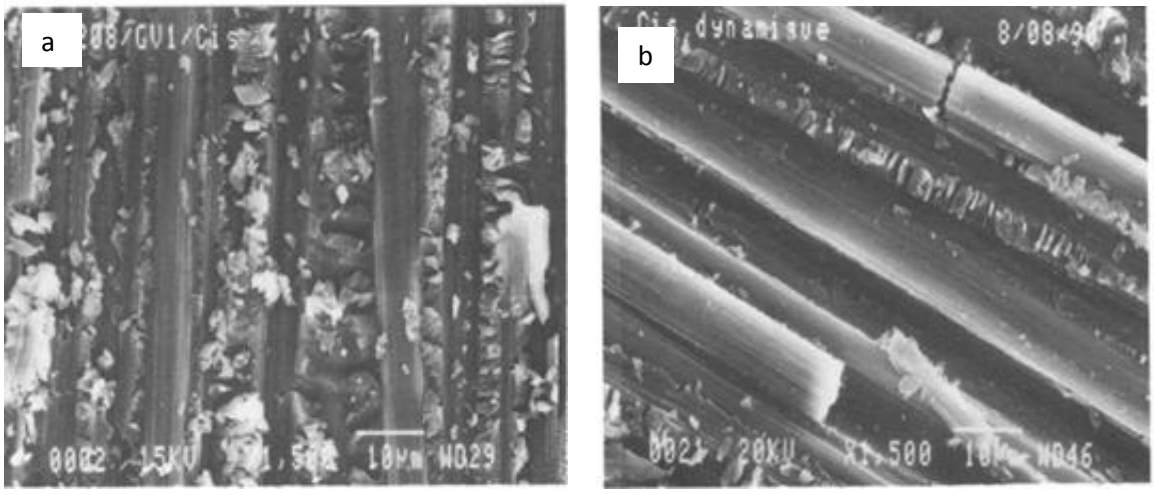

Fig. 2.14 Microphotographs of tested specimen fracture surfaces: (a) and (b) at high strain rate [35].

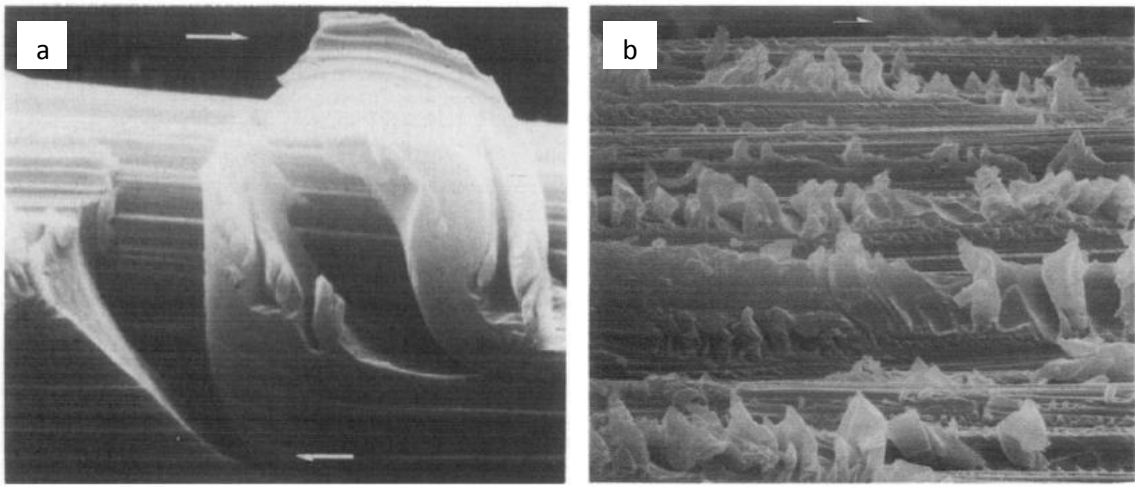

Fig. 2.15 SEM micrographs showing (a) shear cusp (b) cusps on a shear surface for carbon/epoxy composites [37].

2.8 Environmental Implications

Fibrous composites are increasingly being used in many applications owing to various desirable properties including high specific strength, high specific stiffness and controlled anisotropy. But unfortunately, polymeric composites are susceptible to temperature and moisture when operating in changing environmental conditions. For better utilization of these systems comprehensive understanding of the mechanisms of ageing and environmental exposure related deterioration is of immense importance.

2.8.1Effects of Temperature on FRP Composites

Effects of temperature on fibrous polymeric composites are one of the most difficult challenges for neophytes and composite structure designers because it can dramatically change the response of the composite materials. A material that exhibits ductile behavior at room temperature may become brittle at low temperatures or may soften and creep at elevated temperatures [38]. With these temperature fluctuations changes in strength and or stiffness are observed as well. The effect of the combination of thermal and mechanical stresses may well cause a change in mode and location of failure as well as a change in threshold load factor needed to cause failure. It is very difficult to generalize the effect of change of temperature. The matrix dominated properties are such as compressive, flexural, shear and transverse properties are most affected by the temperature dependence on the matrix. Thermal conditioning imparts better adhesion and thus, an improved ILSS value especially at the less conditioning time [39]. When considering the temperature dependence for the physical properties of many polymeric materials, various relaxation effects are extremely important. In polymer molecules a dynamic mechanical relaxation occurs due to heat transfer between the intermolecular mode (strain-sensitive mode) and the intra-molecular mode (strain-insensitive mode) [40]. Thermal degradation of resin involves chemical reaction and physical changes. Chemical reaction is represented by oxidation, further cross-linking and further reaction of un-reacted monomers, while physical change is the visco-elastic behavior [41]. The visco-elastic yield behavior generally depends upon the temperature and loading rate. At the macromolecular scale chain scission and cross-linking affect the polymer network and thus, alter the mechanical properties of the oxidized layer. At the macroscopic level, the hindered shrinkage of the oxidized layer induces a stress gradient susceptible to initiate and propagate cracks [42]. Thermal conditioning behavior of glass/epoxy

and carbon/epoxy composites is of special interest, because of their expanding use for structural applications, where increased temperatures are common environmental conditions. Fracture processes of polymers are strongly influenced by deformation or yielding processes which depend on temperature and time. At very low temperature no yielding is possible and fracture is brittle. At high temperatures two characteristic phenomena occur after the yield point: strain softening and strain hardening. The specimens tested at a lower temperature are characterized by a greater level of micro-cracking and de-lamination. These effects are believed due to higher thermal residual stresses [41]. Due to heterogeneous nature of the fiber and matrix there is large thermal expansion and contraction mismatch which generates thermal stresses. This weakens the fiber/matrix interface as a result their inter-laminar shear strength (ILSS) values deteriorate progressively.

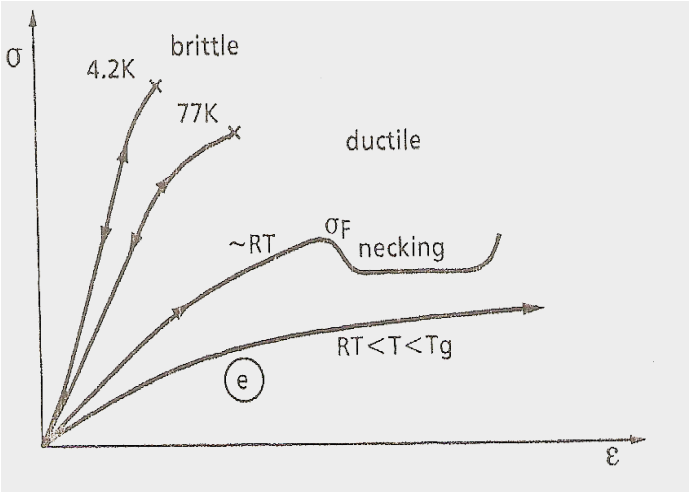

Fig. 2.16 stress-strain curves at different temperatures [24]

2.8.1.1 Effects of temperature on glass transition temperature of polymers

Organic matrix resins such as epoxies soften as the temperature is increased, when it passes through the glass transition (T_g). Above the Tg, the resin exhibit a significant decrease in strength and stiffness due to increased polymer chain mobility [43]. There are several factors which influence the magnitude of the temperature region where the T_g occurs.

1. Composition of the resin molecule
2. Cross link density
3. The polar nature of the resin molecules functional groups
4. Curing agent or the catalyst
5. Cure time and temperature

2.8.1.2 Effect of T_g on mechanical properties

T_g is used for evaluating the flexibility of a polymer molecule and the type of response the polymeric material would exhibit to mechanical stress. Polymers above their T_g will exhibit a delayed elastic response (visco-elasticity), while those above T_g will exhibit dimensions stability. General commonsense prevails that higher the T_g better the mechanical properties.

2.8.2 High Temperature

Thermal conditioning at above ambient temperature might possibly improve adhesion level at the interfaces. Adhesion chemistry at the interface may be influenced by post-curing phenomena and this effect is supposed to increase with more conditioning time limited by some optimum value [39]. Thermal conditioning caused matrix shrinkage due to volatile loss and additional cure of matrix [44]. Glass/epoxy composite plate's losses their rigidity and strength at room temperature and high temperatures (40, 60, 80, and 100˚C) [45]. However, the fracture behavior and mechanism of the CFRP composites at high-temperature levels are complicated when compared with those of the composite at room temperature; the fracture process is characterized by fiber breakage, fiber/matrix interfacial fracture, and de-lamination occurred between adjacent plies of the laminates. Inter-laminar shear strengths decrease nearly linear by increasing temperature [46]. At high temperatures above the glass transition temperature (T_g), polymer composites are susceptible to thermo-oxidative degradation. Although the fibers are stable below T_g but the matrix and especially the fiber–matrix interface can undergo degradation that affects the physical and mechanical properties of the composite structures over time [47]. Thermal conditioning is to induct further polymerization process with the development of penetrating and/or semi-penetrating network at the fiber/matrix interface. The response of fiber/matrix interface within the composite plays an important role in determining the gross mechanical performance, because it transmitting the load from the matrix to the fibers, which contribute the greater portion of the composite strength. Better the interfacial bond better will be the ILSS, de-lamination resistance, fatigue and corrosion resistance.

2.8.3 Low Temperature

The cryogenic properties of polymers are required in space, superconducting magnet and electronic technologies. Potholing or localized surface degradation, de-lamination, and micro

cracking are some of the more dramatic phenomena that can occur as a result of cryogenic cycling [48]. Compressive residual stresses developed due to differential thermal contraction, influence the overall thermo-mechanical properties of the composite. In some cases, the resulting stresses are sufficient to initiate plastic deformation within the matrix immediately around the fiber. The thermal residual stresses can also be large enough to initiate material damage such as matrix micro cracking. These micro cracks can reduce both the stiffness and the strength of the material, as well as act as sites for environmental degradation and nucleation of macro cracks [49]. The propensity for micro-cracking and the micro-crack morphology depends on the type of fiber and matrix used [50]. At low temperature the cross-linked polymers shows brittle behavior and it don't allow relaxation of the thermal residual stresses.

2.8.4 Effects of Moisture

The degree of environmental degradation that occurs in a fiber reinforced polymer composite structure is linked directly with the amount of moisture that is absorbed. The rate of absorption of water can be successfully predicted by Fick's law of diffusion, where moisture content at any instant of time is proportional to the square root of time for $Dt/h^2 < 0.05$. When the diffuse water molecules wander in a random manner through the composite, absorption characteristics in this case can be described by Langmuir's two phase model, also called modified diffusion model. But the moisture absorption kinetics of epoxy resins differs widely and also changes with physical ageing. Moisture may penetrate into polymeric composite materials by diffusive and /or capillary processes [51-53].

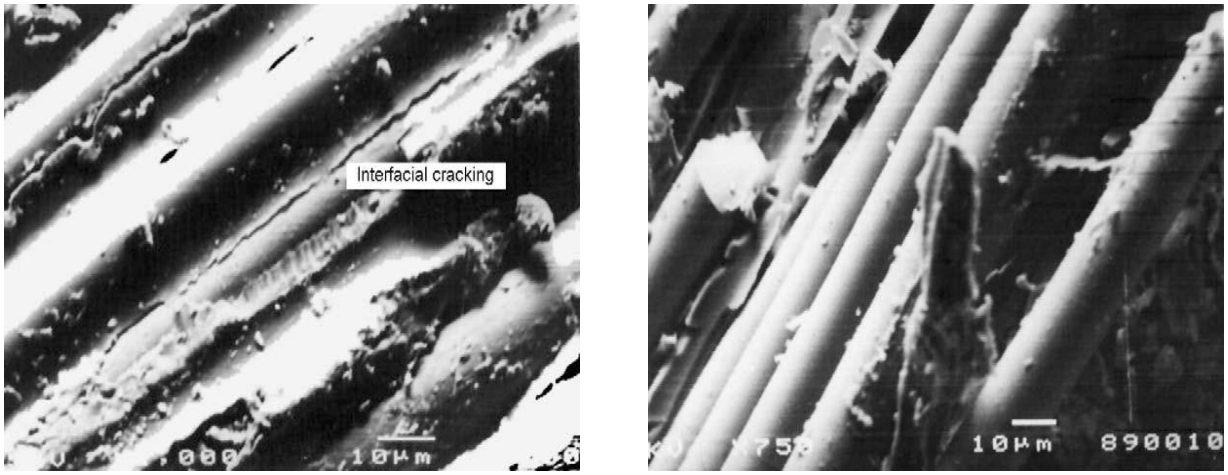

Fig.2.17 De-adherence and interfacial cracking is evident in aged glass/epoxy laminated composites [54]

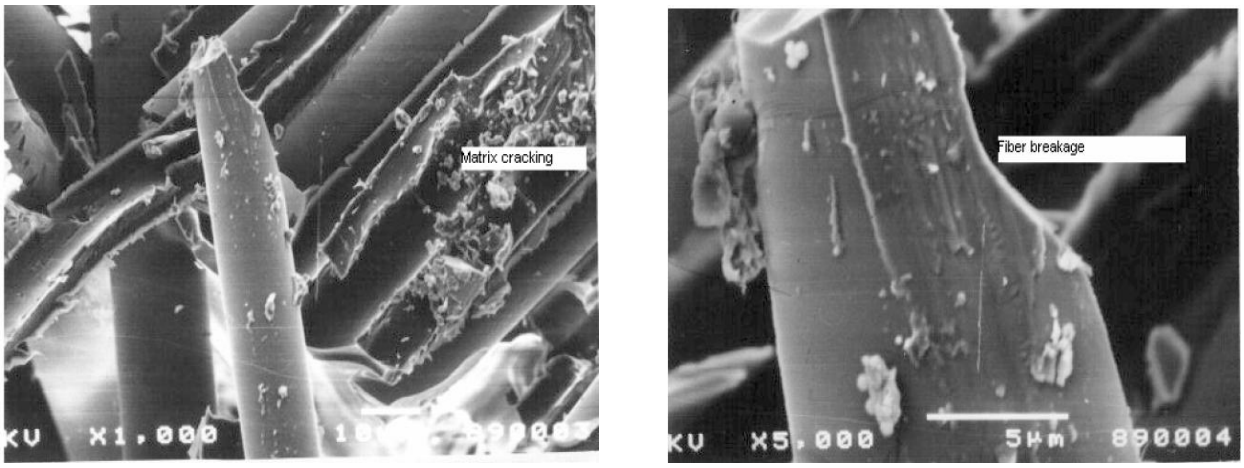

Fig.2.18 scanning electron micrograph shows matrix cracking and fiber damage in carbon/epoxy composites [54].

Summary of literature review

From the present review it has been shown that due to the presence of the relatively stiff fibers increases the influence of shear stresses on the resin facture particularly in the production of cusps. The detailed investigation of the micro structural analysis of glass- and carbon- fiber reinforced epoxy composites; matrix fracto-graphic analysis has thrown new lights on the failure mechanism.

CHAPTER 3

MATERIALS AND METHODS

MATERIALS

EXPERIMENTAL METHODS

EXPERIMENTAL PROCEDURE

Chapter 3

3. Materials and Methods

3.1 Materials

Resin LY-556 is an unmodified liquid epoxy resin based on Bisphenol A along with Hardener HY 951(aliphatic primary amine), it provides a low viscosity, solvent free room temperature curing laminating system. Silane treated woven roving E-glass fibers with 60 weight percentages were used for glass/epoxy composite fabrication. Woven carbon fibers of epoxy compatible sizing (PAN based high strength) with 60 weight percentages were used for fabrication of carbon/epoxy composites.

3.2Experimental Methods

3.2.1Flexural Test (Short beam shear test)

The flexural methods are applicable to polymeric composite materials. A testing machine with controllable crosshead speed is used in conjunction with a loading fixture. It is a three point flexural test on a specimen with a small span, which promotes failure by inter-laminar shear [55]. The shear stress induced in a beam subjected to a bending load, is directly proportional to the magnitude of the applied load and independent of the span length. Thus the support span of the short beam shear specimen is kept short so that an inter-laminar shear failure occurs before a bending failure.

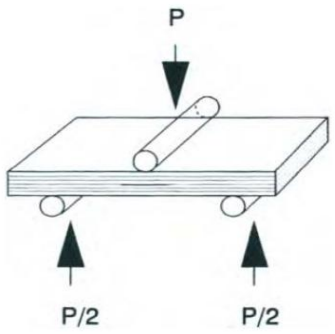

Fig. 3.1 Schematic of loading configuration of short beam shear test

This test method is defined by ASTM D 2344, which specifies a span length to specimen thickness ratio of five for low stiffness composites and four for higher stiffness composite. This test has an inherent problem associated with the stress concentration and the non-linear plastic deformation induced by the loading nose of small diameter. This is schematically illustrated in fig 3.2, where the effects of stress concentration in a thin specimen are compared with those in a thick specimen. Both specimens have the same span-to-depth ratio (SDR). The stress state is much more complex than the pure shear stress state predicted by the simple beam theory.

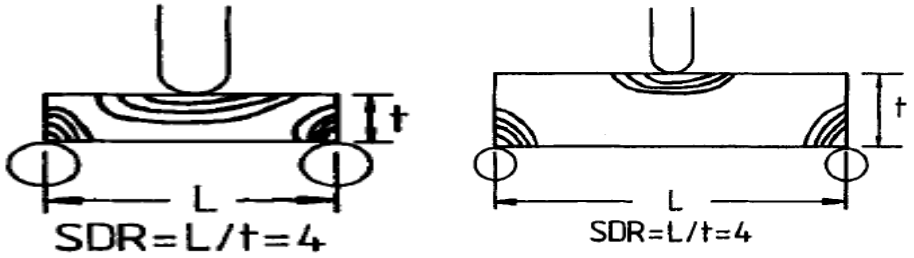

Fig.3.2 Effect of stress concentrations on short beam shear specimens: (a) thin specimen; (b) thick specimen [9].

According to the classical beam theory, the shear stress distribution along the thickness of the specimen is a parabolic function that is symmetrical about the neutral axis where it is at its maximum and decreases toward zero at the compressive and tensile faces. In reality, however, the stress field is dominated by the stress concentration near the loading nose, which completely destroys the parabolic shear distribution used to calculate the apparent ILSS. Recognizing the deficiencies many investigators performed detailed study of this test method.

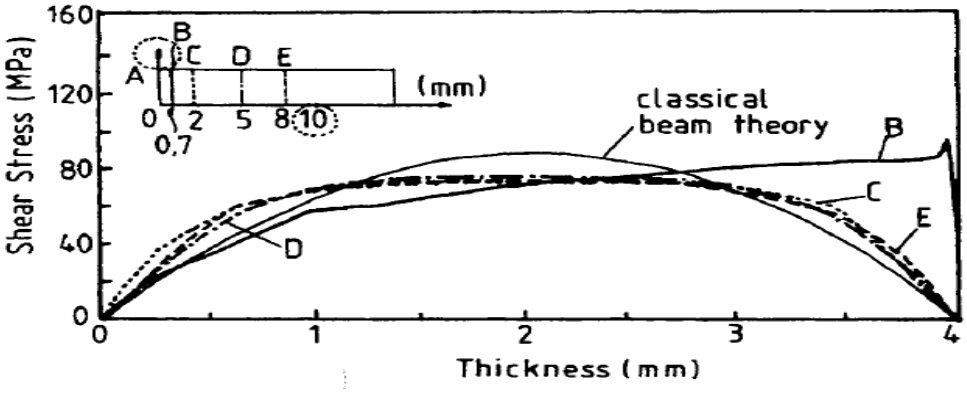

Fig. 3.3 Shear stress distributions across the thickness of a three-point bending specimen in a short beam shear test [9]

They observed that by significantly increasing the diameters of the support and loading cylinders and increasing the span to length thickness ration to about eight. With these variations the results shows that the parabolic distribution of shear stress across the thickness of the specimen predicted by simple beam theory could be very well in the regions between the loading and support cylinder and the specimen fail in a shear mode [56]. With these modifications ASTM D 2344 may yet become a technically acceptable as well as popular shear test method

3.2.2 Scanning Electron Microscope (SEM)

The scanning electron microscope (SEM) has been a well accepted tool for many years in the examination of fracture surfaces. The prominent imaging advantages are the great depth of field and high spatial resolution and the image is relatively easy to interpret visually.

Principle: A finely focused electron beam scanned across the surface of the sample generates secondary electrons, backscattered electrons, and characteristic X-rays. These signals are collected by detectors to form images of the sample displayed on a cathode ray tube screen. Features seen in the SEM image may then be immediately analyzed for elemental composition using EDS or WDS. The electrons that are emitted from the specimen surface have a spectrum of energies. Secondary and backscattered electrons are conventionally separated according to their energies. When the energy of the emitted electron is less than about 50eV, it is referred as a secondary electron and backscattered electrons are considered to be the electrons that exit the specimen with energy greater than 50eV. A critical point in understanding the formation of SEM images of fracture surfaces, and their interpretation, is an appreciation of the factors that affect this excited volume of electrons in the specimen [57]. To understand the different failure mechanisms in FRP composites, photomicrographs were taken using a SEM. There is a dramatic change in the structure and properties of the composite when exposed to high and low temperatures.

3.2.3 Differential Scanning Calorimetry (DSC)

Principle: Differential scanning calorimetry (DSC) is a thermoanalytical technique in which the amount of heat required to increase the temperature of a sample and reference is measured as a function of temperature. Both the sample and reference are maintained at nearly the same temperature throughout the experiment.

3.2.4 FTIR Spectroscopy analysis

Principle: In infrared spectroscopy, Infrared radiation is passed through a sample. Some of the infrared radiation is absorbed by the sample and some of it is passed through (transmitted). The resulting spectrum represents the molecular absorption and transmission, creating a molecular fingerprint of the sample. Like a fingerprint no two unique molecular structures produce the same infrared spectrum. This makes infrared spectroscopy useful for several types of analysis. Infrared spectroscopy is useful in the region to get structural information for organic compounds. This region is divided into two parts i.e. the functional group region 4000-1300 cm^{-1} and 1300-650 cm^{-1} finger print region. Most of the functional groups give absorption bands in the high frequency part of the spectrum, which give small number of bands [58]. The FTIR image analysis suggests that there is a variation in the chemical structure of the matrix from the fiber to the bulk polymer [59].

3.2.5 Atomic force Microscopy (AFM)

Principle: The AFM consists of a cantilever with a sharp tip (probe) at its end that is used to scan the specimen surface. The cantilever is typically silicon or silicon nitride with a tip radius of curvature on the order of nanometers. When the tip is brought into proximity of a sample surface, forces between the tip and the sample lead to a deflection of the cantilever according to Hookes law. AFM has become a useful tool for characterizing the topography and properties of solid materials since its advent. Besides topography information, the phase lag of the cantilever oscillation, relative to the signal sent to the cantilever's piezo driver, is simultaneously monitored giving information about the local mechanical properties such as adhesion and viscoelasticity. Phase imaging is a powerful tool that provides nanometer-scale information often not revealed by other microscopy techniques [32].

3.3 Experimental Procedure

Glass/epoxy composite laminates were fabricated by hand lay-up method, silane treated E-glass fiber of required dimensions was laid over a releasing sheet and then catalyzed epoxy resin was poured absorbed over the reinforcement. The wet composite was rolled, to distribute the resin and to remove the air pockets. The sequence was repeated until the desired thickness was

obtained. The layered structure was allowed to harden on cure. It was cured at room temperature for 48 hours. After curing, the laminate was cut into the required size for 3-point bend (Short-Beam Shear) test by diamond cutter. Then stability test was done for the composite laminates. Here the laminates were weighed and then heated in an oven at 50˚C. The weight is intermittently checked till we get a stable weight, so that with further heating of the composites there is no change in the weight. The same procedure was again repeated for the fabrication of carbon/epoxy laminates.

3.3.1Thermal conditioning:

3.2.1.1Above ambient temperature

One batch of sample was put in a baking oven at +50˚C for 2 and 5 hours for thermal conditioning at above ambient temperature.

3.2.1.2Below ambient temperature

Similarly another batch of sample was put in an ultra low chamber at -50˚C for 2 and 5 hours conditioning time.

3.2.1.3Above the glass transition temperature (T_g)

For thermal conditioning at above the glass transition temperature, one batch of glass/epoxy specimen were heated at +80˚C for 2 hours. The samples were cooled again when they acquired ambient temperature tested in 3-point bend test.

3.3.2 Short beam shear test

The short beam shear (SBS) tests are performed on the composite samples at the conditioned temperature and room temperature to evaluate the value of inter-laminar shear strength (ILSS). It is a 3-point bend test, which generally promotes failure by inter-laminar shear. The SBS test is conducted as per the ASTM standard D2344-84 with an Instron 1195 tensile testing machine fig.3.5 (a). The loading arrangement is shown in figure 4.1(b) a span length of 40 mm .The tests were performed with five increasing crosshead speed ranging from 1, 10,100, 200 and 500 mm/min. For each point of testing 4 to 5 specimen were tested and the average value was taken.

(a)

(b)

Fig. 3.5 Instron 1195 with short beam shear test set up, loading of the sample and fracture

mm/min

1

10

100

200

500

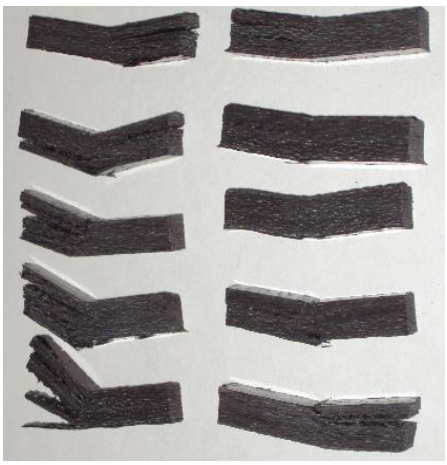

Fig. 3.6 Glass/epoxy and carbon/epoxy tested samples at different crosshead speeds

3.3.3SEM Analysis

To study the different failure mechanisms of the tested samples micrographs of the failure samples was carried out using a JEOL-JSM 6480 LV SEM. The samples were loaded onto the sample holder and placed inside the SEM, adjusting the working distance and hence the spot size the chamber was closed and vacuum was applied.

3.3.4 DSC Analysis

The DSC measurements were performed on a Mettler-Toledo 821 with intra cooler, using the STAR software. The temperature calibration and the determination of the time constant of the instrument were performed by standards of In and Zn, and the heat flow calibration by In. The underlying heating rate of 10˚Cmin-1 was used. In order to calibrate the heat flow signal, a blank run with an empty pan on the reference side and an empty pan plus a lid at the sample side was performed before the sample measurements. Standard aluminum pans were used. The experiments were performed in the temperature range from 25˚C to 120˚C.

Fig. 3.7 Mettler -Toledo 821 with intra cooler for DSC measurements and reference sample chamber

3.3.5 FTIR Analysis

FTIR analysis was performed in FTIR spectrophotometer interfaced with IR microscope operated in reflectance mode. The microscope is having a video camera, a liquid nitrogen-cooled mercury cadmium telluride (MCT) detector and a computer controlled translation stage, programmable in the x and y directions. The spectra were collected in the 4000cm^{-1} to 650 cm^{-1} region with 8 cm^{-1} resolution, 60 scans and beam spot size of 20µm- 100µm. The spectral point-by-point mapping of the interface of the epoxy cured composites was performed in a grid pattern

with the use of computer controlled microscope stage. Since the surface of the film was not perfectly smooth and its thickness was not uniform care should be taken to mount the sample such that a major portion of the plane was in the same focal plane. The FTIR imaging was performed in AIM-800 Automatic Infra red Microscope (SHIMADZU).

Fig. 3.8 (a) FTIR spectrophotometer, (b) AIM-800 Automatic Infra red Microscope

3.3.6 AFM

The surface polished specimens of glass/epoxy and carbon/epoxy composites were exposed in a thermal conditioning environment at 50˚C for different time period. After thermal conditioning the specimens were put in desiccators to protect them from moisture and dust. The specimens were taken out of the desiccators periodically and then scanned by Veeco Dinnova atomic force microscope

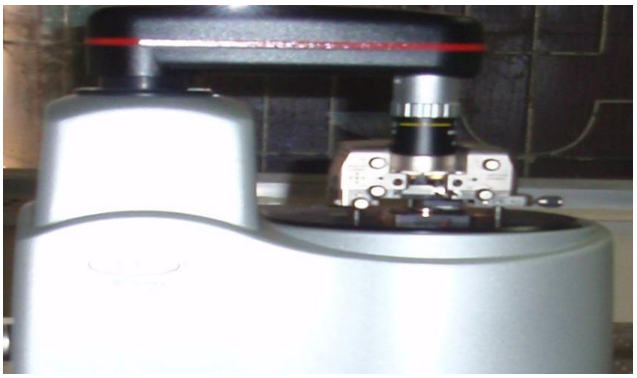

Fig. 3.9 Model of Veeco Dinnova atomic force microscope

CHAPTER 4

RESULTS AND DISCUSSION

1. Fibrous polymeric composites under different loading speeds at above- and sub-ambient temperatures

2. Effects of Temperature and Loading Speed on Inter-laminar Strength of FRP Composites

Chapter 4

4. Results and Discussion

4.1 Fibrous polymeric composites under different loading speeds at above- and sub- ambient temperatures

4.1.1Short Beam Shear Test:

After short beam shear test at the conditioning temperature of the thermal conditioned samples

The ILSS values are calculated as:

ILSS = 0.75P/bd

Where, P is maximum load, b the width of specimen and d the thickness of specimen

4.1.1.1Glass/epoxy composites

The variation of ILSS values for both the conditioned specimens are plotted against the cross head speeds for glass/epoxy composites in fig 4.1(a) at above ambient and fig 4.2(a) at sub ambient temperatures. It is a three-point flexural test, which generally promotes failure by inter-laminar shear, and the results of the test are useful for assessment of interfacial de-bonding and composite quality [60]. Fig 4.1(a) depicts the ILSS value increases at each point of testing with increasing temperature and time. Due to thermal conditioning at above ambient temperature, there is further polymerization in terms of epoxy embrittlement and along with the development of penetrating and/or semi-penetrating network at the fiber/matrix interface. At lower cross head speed the polymer gets more time for relaxation, less gross plastic deformation, enhancement of ILSS. With increasing cross head speed up to 100mm/min crack density increases due to structural integrity losses, this deteriorates ILSS values. At higher cross head speed there is shorter load assisted relaxation time, the polymer unable to transfer the load properly, reduction in ILSS. Here the load is like an impact due to this several damage mechanisms such as fiber fracture, fiber pull out, matrix cracking and de-lamination occur. These micro-failure processes allow a composite laminate to exhibit a more gradual deterioration rather than a catastrophic failure [4].

Table 4.1 ILSS Vs. Crosshead speed for glass/epoxy composites at +50˚C for 2 and 5 hours conditioning time

Crosshead speed	ILSS at ambient	ILSS at +50˚C for 2hrs	ILSS at +50˚C for 5hrs
1	18.5	22.51	24.98
10	17.84	19	22.82
100	17.26	18.42	22.4
200	18.03	19.77	20.56
500	18.36	20.05	21.88

Table 4.2 Strain at yield Vs. Crosshead speed for glass/epoxy at +50˚C for 2 and 5 hours conditioning time

Crosshead speed	Strain at yield at ambient	Strain at yield at +50˚C for 2hrs	Strain at yield at +50˚C for 5hrs
1	0.032	0.0322	0.0342
10	0.0219	0.023	0.0267
100	0.0126	0.0122	0.0085
200	0.0289	0.0318	0.0131
500	0.041	0.0543	0.0372

Table 4.3 ILSS Vs. Crosshead speed for glass/epoxy at -50˚C for 2 and 5 hours conditioning time

Crosshead speed	ILSS at ambient	ILSS at -50˚C for 2hrs	ILSS at -50˚C for 5hrs
1	18.5	24.39	23.16
10	17.84	25.84	27.05
100	17.26	25.2	26.07
200	18.03	27.72	27.34
500	18.36	26.38	25.68

Table 4.4 Strain at yield Vs. Crosshead speed for glass/epoxy composites at -50˚C for 2 and 5 hours conditioning time

Crosshead speed	Strain at yield at ambient	Strain at yield at -50˚C for 2hrs	Strain at yield at -50˚C for 5hrs
1	18.5	24.39	23.16
10	17.84	25.84	27.05
100	17.26	25.2	26.07
200	18.03	27.72	27.34
500	18.36	26.38	25.68

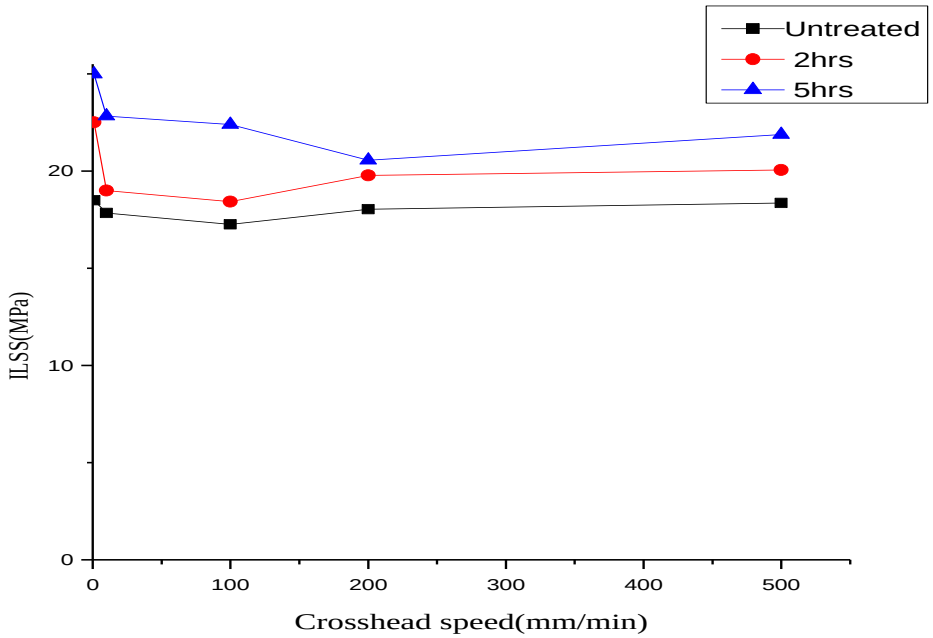

Fig.4.1 (a) ILSS Vs Crosshead speed for Glass/epoxy composites above ambient temperature at + 50˚C for 2 and 5 hours conditioning time

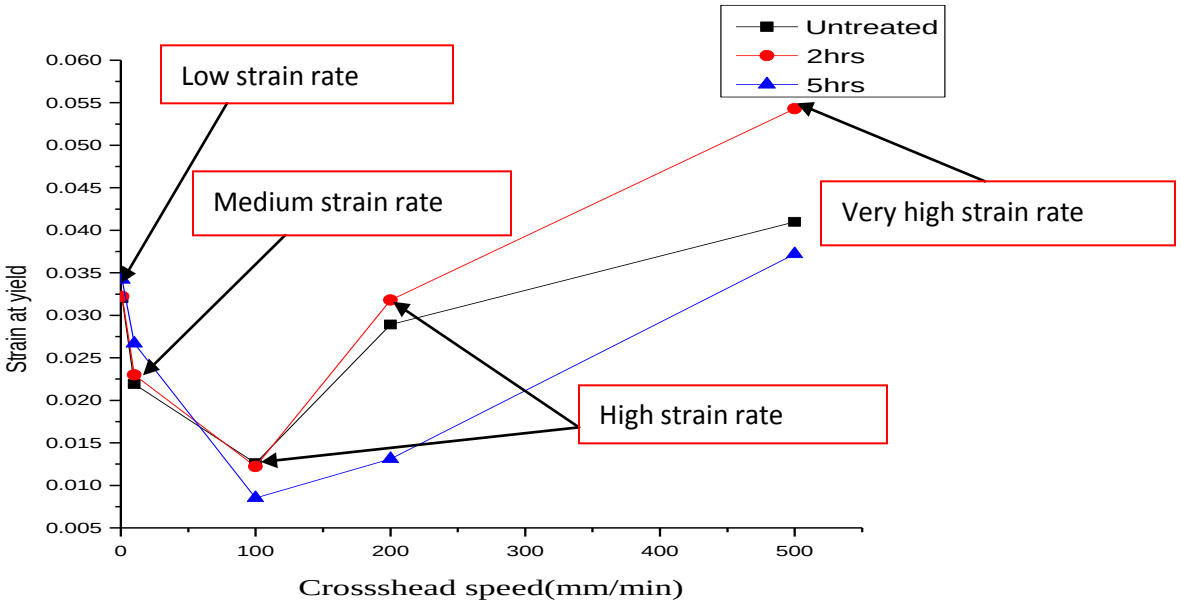

Fig.4.1 (b) Strain at yield Vs Cross head speed for Glass/epoxy composites above ambient temperature at + 50˚C for 2 and 5 hours conditioning time

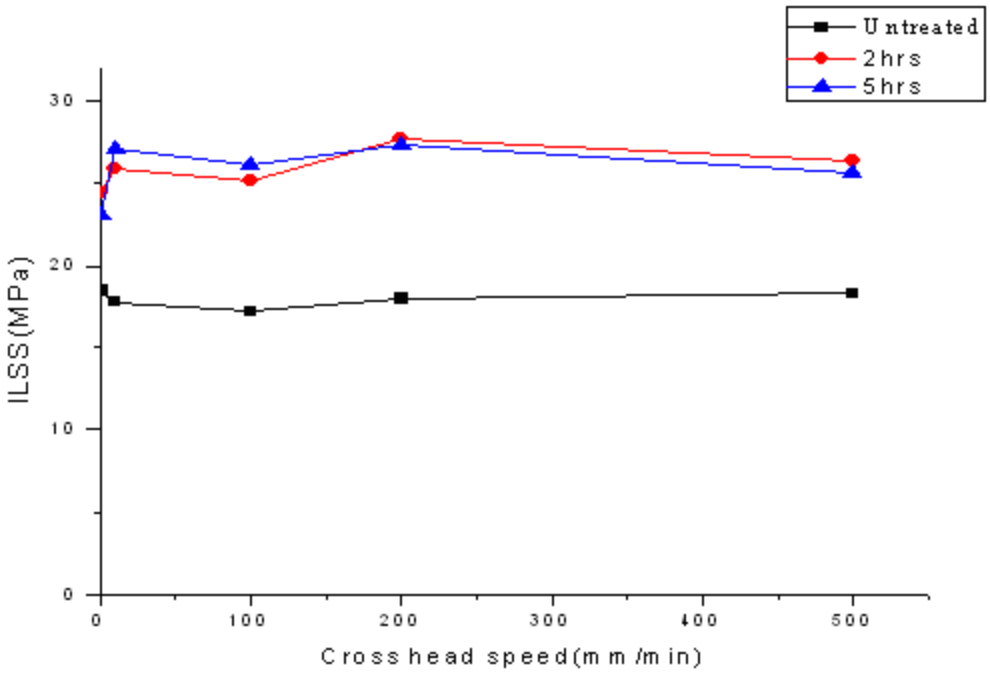

Fig.4.2 (a) ILSS Vs Crosshead speed for Glass/epoxy composites below ambient temperature at -50˚C for 2 and 5 hours conditioning time

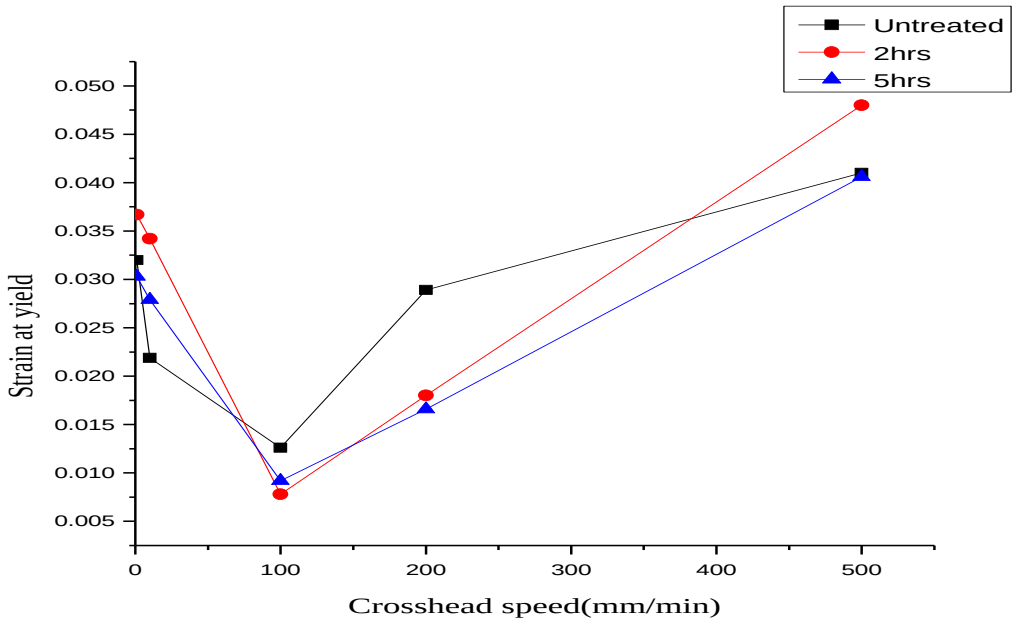

Fig.4.2 (b) Strain at yield Vs Crosshead speed for Glass/epoxy composites below ambient temperatures at -50˚C for 2 and 5 hours conditioning time

Fracture processes at the crack tip of polymers are controlled by mechanical and thermal relaxation time. At low strain rate loading time greater than mechanical relaxation time and at high strain rate loading time greater than thermal relaxation time [24]. Fig. 4.1(b) prevails that at lower stain rate the polymer becomes brittle, less plastic deformation which results higher strain at yield values and at higher strain rate the strain at yield increases due to adiabatic heating i.e. here heat generation was faster than heat removal at the time of testing. The results obtained from fig.4.2(a) depicts due to low temperature exposure compressive stresses are developed which improves the lock and key adhesion mechanism at the fiber matrix interface, epoxy resin opens more despite of the low temperature hardening. Crack density is less likely to occur as compared to thermal conditioning above ambient temperature as a result there is improvement of ILSS values. Thermal conditioning at above ambient temperature might possibly improve adhesion level at the interfaces. Adhesion chemistry at the interface may be influenced by post-curing phenomena and this effect is supposed to increase with more conditioning time limited by some optimum value. Fig.4.2(b) showing that at higher crosshead speed i.e. at 500 mm/min the strain at yield is higher for 2 hours conditioning time.

4.1.1.2Carbon/epoxy Composites

The effect of cross head speeds on ILSS for carbon/epoxy composites at above ambient showing fig.4.3 (a) there is increase in ILSS values with more thermal conditioning time; it may be due to post curing. From fig.4.4(a) it has been observed that carbon/epoxy composites at below ambient temperature shows lower ILSS than ambient temperature, at low temperature the carbon fibers contracts in the transverse direction and expands in longitudinal direction simultaneously with the contraction of epoxy matrix in all directions[61]. As a result there may be weaker interfacial bond between carbon fiber and epoxy matrix below ambient temperature. Strain at yield Vs cross head speed for carbon/epoxy systems at above ambient fig 4.3(b) and below ambient temperature fig 4.4(b) are vary in a similar fashion as glass/epoxy systems. Where as at below ambient, carbon/epoxy systems shows less ILSS properties due to higher matrix cracking manifested by low temperature resin hardening. At the above ambient temperature due to further polymerization, interfacial strength increases. The locus of failure will shift from fiber polymer interface to the matrix itself that means instead of adhesion failure the predominating failure may be cohesive failure and that too shear cusp formation.

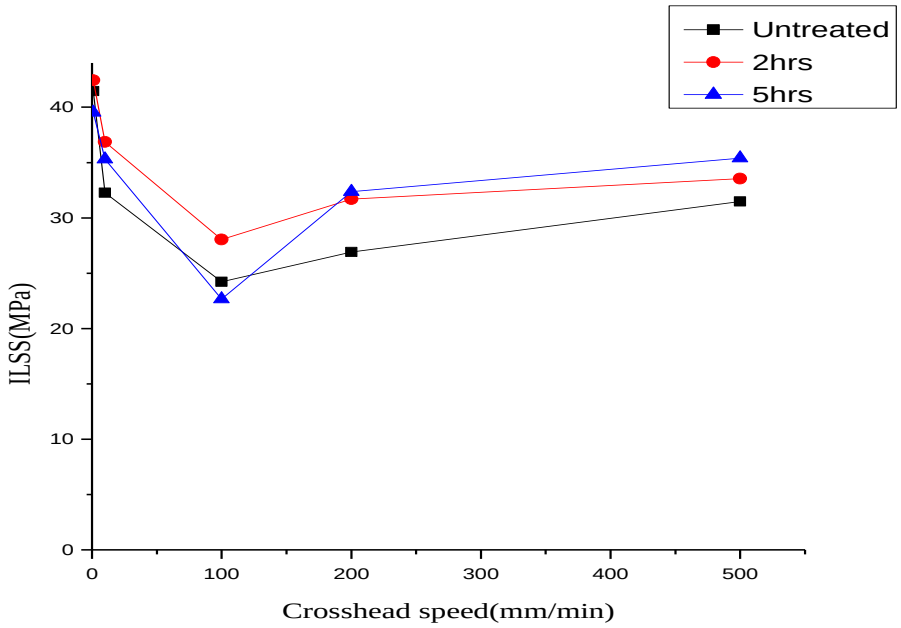

Fig.4.3 (a) Crosshead speed Vs ILSS for carbon/epoxy composites above ambient temperature at + 50˚C for 2 and 5 hours conditioning time

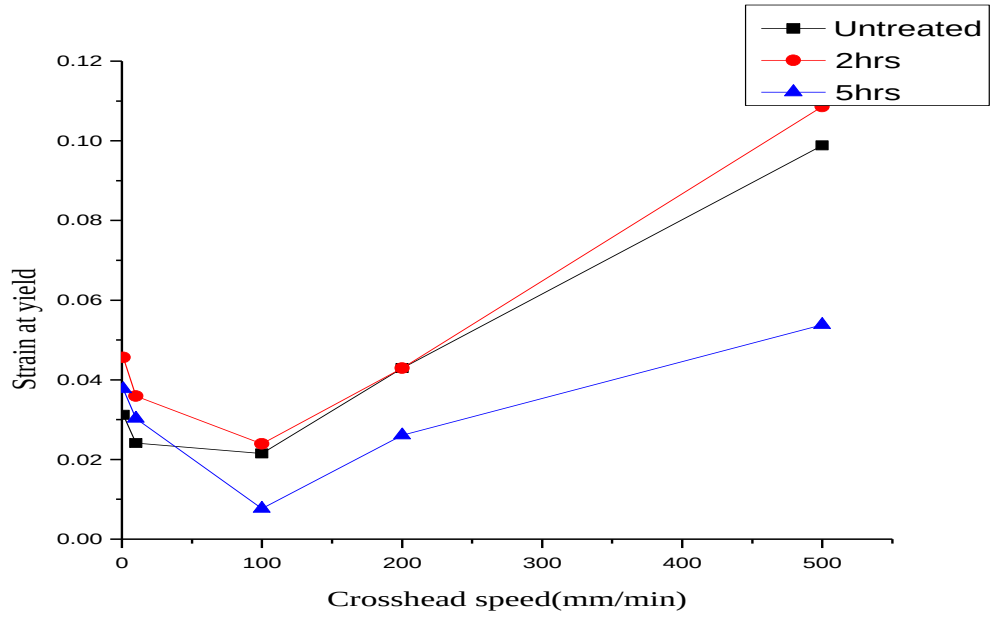

Fig.4.3 (b) Strain at yield Vs Crosshead speeds of carbon/epoxy composites above ambient temperatures at + 50˚C for 2 and 5 hours conditioning time

Table 4.5 ILSS Vs. Crosshead speed for carbon/epoxy composites at +50˚C for 2 and 5 hours conditioning time

Crosshead speed	ILSS at ambient	ILSS at +50˚C for 2hrs	ILSS at +50˚C for 5hrs
1	41.46	42.43	39.53
10	32.28	35.29	36.86
100	24.22	28.04	22.67
200	26.91	31.69	32.38
500	31.47	33.55	35.39

Table 4.6 Strain at yield Vs. Crosshead speed for carbon/epoxy composites at +50˚C for 2 and 5 hours conditioning time

Crosshead speed	Strain at yield at ambient	Strain at yield at +50˚C for 2hrs	Strain at yield at +50˚C for 5hrs
1	0.0312	0.0456	0.0377
10	0.0241	0.0359	0.0303
100	0.0215	0.0239	0.0077
200	0.0429	0.0429	0.0261
500	0.0988	0.1086	0.0538

Table 4.7 ILSS Vs. Crosshead speed for carbon/epoxy composites at -50˚C for 2 and 5 hours conditioning time

Crosshead speed	ILSS at ambient	ILSS at -50˚C for 2hrs	ILSS at -50˚C for 5hrs
1	41.46	32.38	41.22
10	32.28	28.83	32.89
100	24.22	22.86	23.69
200	26.91	23.78	24.02
500	31.47	29.45	31.75

Table 4.8 Strain at yield Vs. Crosshead speed for carbon/epoxy composites at -50˚C for 2 and 5 hours conditioning time

Crosshead speed	Strain at yield at ambient	Strain at yield at -50˚C for 2hrs	Strain at yield at -50˚C for 5hrs
1	0.0298	0.0312	0.0331
10	0.0215	0.0252	0.0299
100	0.0157	0.0215	0.0085
200	0.0176	0.0429	0.0148
500	0.0306	0.0988	0.0505

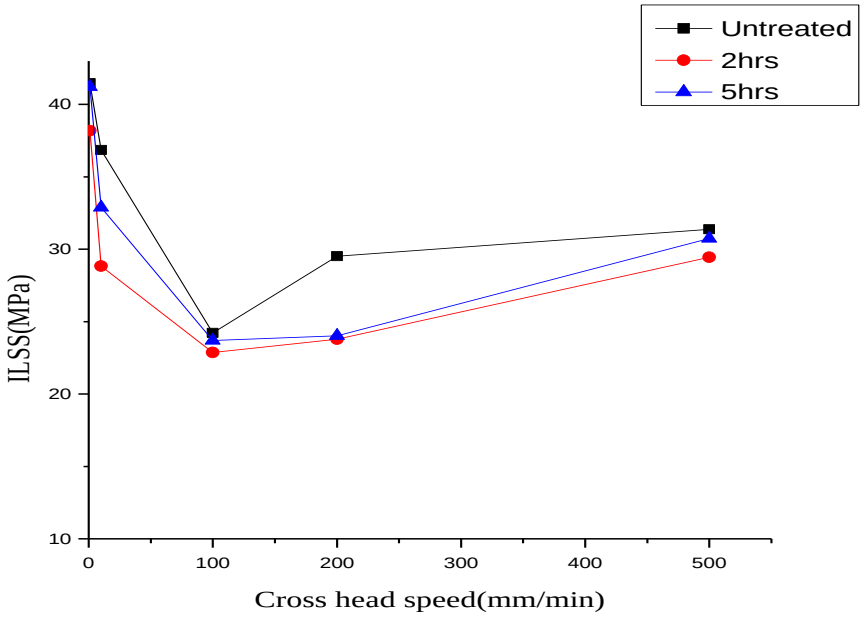

Fig.4.4 (a) Crosshead speed Vs ILSS of carbon/epoxy composites below ambient temperature at -50˚C for 2 and 5 hours conditioning time

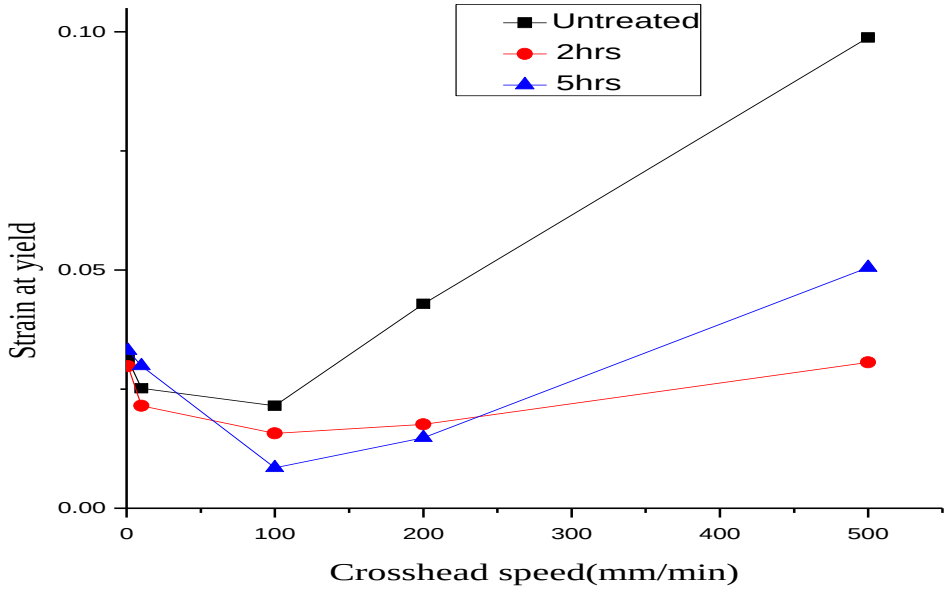

Fig.4.4 (a) Strain at yield Vs Crosshead speed of carbon/epoxy composites below ambient temperatures at -50˚C for 2 and 5 hours conditioning time

4.1.2 Failure analysis by SEM

Due to large thermal expansion and contraction mismatch there is nucleation of fiber matrix de-bonding at the fiber matrix interface. Failure in fiber composite initiates from small defects such as broken fibers, de-bonded interfaces and matrix pores. As the crack propagates due to large transverse tensile stress and interfacial shear stress there is fiber/matrix de-bonding in case of unidirectional composites and inter-laminar cracking or de-lamination in multilayer composites. Behind the crack tip the fibers are pulled out from the matrix, fiber pull-out is an effective energy absorbing mechanism. At higher cross head speed the damage mechanisms are fiber fracture, fiber pull out, matrix cracking and de-lamination occur. These micro-failure processes allow a composite laminate to exhibit a more gradual deterioration rather than a catastrophic failure.

4.1.2.1Glass/epoxy Composites

SEM micrographs of different failure mechanism of glass/epoxy composites are shown in fig.4.5 (a) and (b). Scanning electron micrographs reveals that at higher cross head speed there is extensive fiber pullout and fiber/matrix de-bonding for glass/epoxy composite which demonstrated in fig 4.6(a). Thermal conditioning at below ambient temperature causes differential contraction and increases the resistance to de-bonding by mechanical keying factor. Fig.4.6 (b) reveals the presence of less fiber/matrix de-bonded areas which indicates an enhanced adhesion by thermal condition at below ambient temperature.

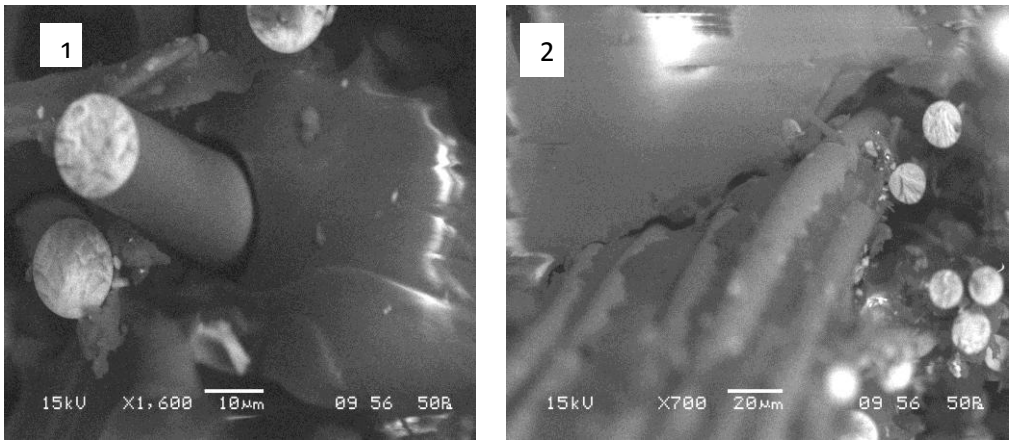

Fig.4.5 (a) SEM micrographs showing (1) fiber/matrix de-bonding, (2) matrix cracking

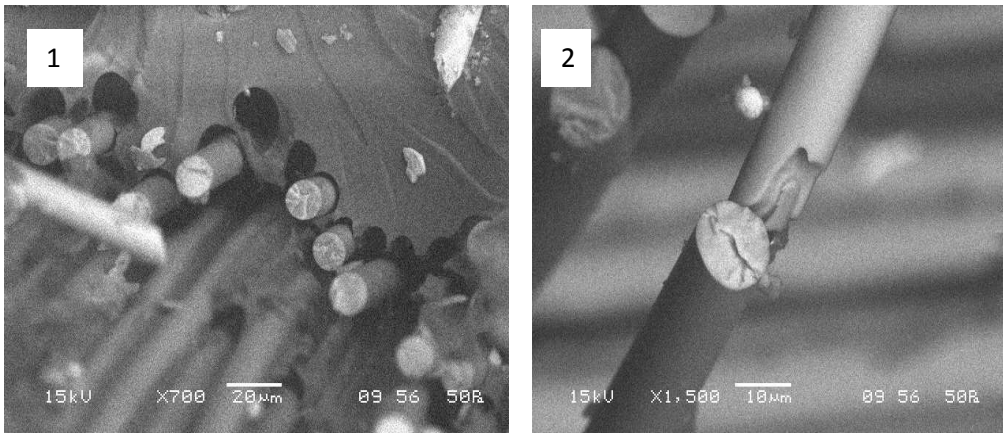

Fig.4.5 (b) SEM micrographs showing (1) fiber pull-out and (2) brittle failure in glass/epoxy composite

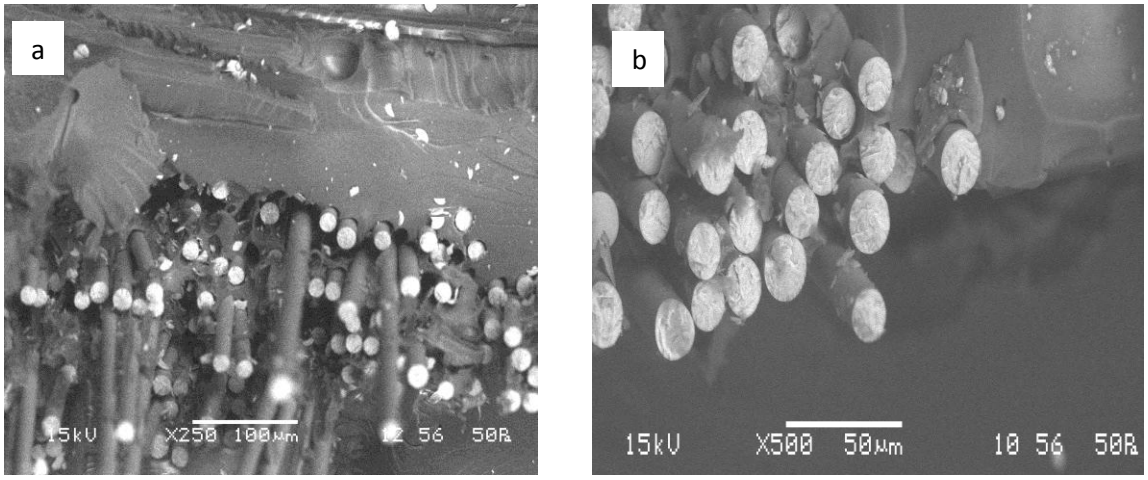

Fig.4.6 (a) Showing extensive fiber/matrix de-bonding and fiber pullout in glass/epoxy composite at higher cross head speed and fig.(b) depicts increase fiber/matrix adhesion at below ambient temperature, less fiber pull-out and de-bonded areas

4.1.2.2Carbon/epoxy Composites

CFRP are sensitive to temperature variations as a result of the development of the thermal stresses between the fibers and matrix due to their distinct thermal expansion coefficients. The induced thermal stresses may be relieved by crack formation in the matrix and in extreme cases, by fiber failure. Both matrix cracking and fiber failure degrade the mechanical properties of the composite. At higher cross head speed there is extensive fiber pullout and fiber/matrix de-bonding, which demonstrated by fig.4.7 (a) for carbon/epoxy composites. Fig.4.7 (b) reveals that adhesion level increase and less de-bonded areas with thermal conditioning for carbon/epoxy

systems. Fig.4.8 (a) depicts signs of few hackle markings for carbon/epoxy and fig.4.8 (b) for glass/epoxy due to thermal conditioning at above ambient temperatures.

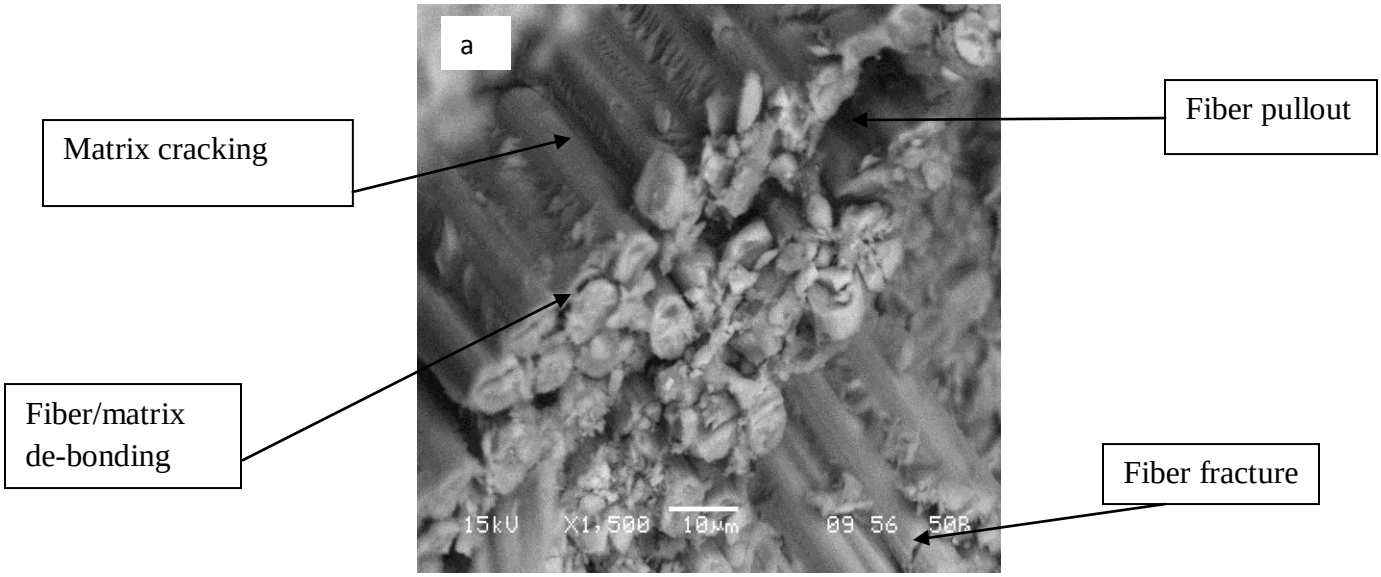

Fig.4.7 (a) Showing matrix cracking, fiber/matrix de-bonding, fiber fracture and fiber pullout at higher cross head speed

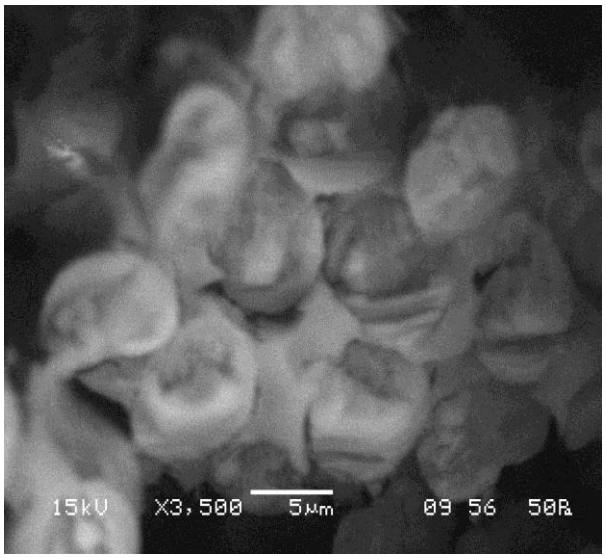

Fig4.7 (b) Depicts increase fiber/matrix adhesion at below ambient temperature, less fiber pull-out and de-bonded areas in carbon/epoxy composites

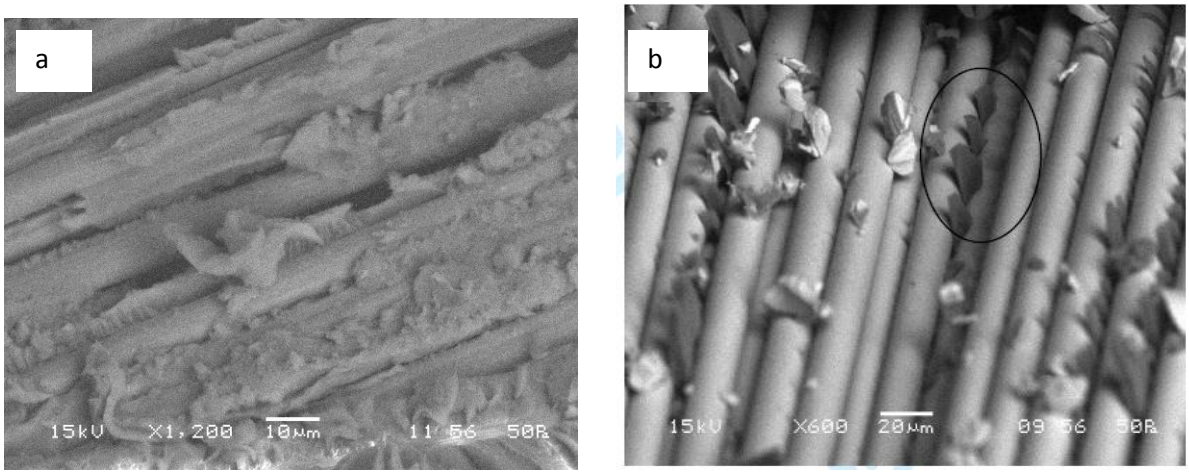

Fig.4.8 (a) represents fracture surface of carbon/epoxy and (b) glass/epoxy composite specimens showing few hackle markings (shear cusp)

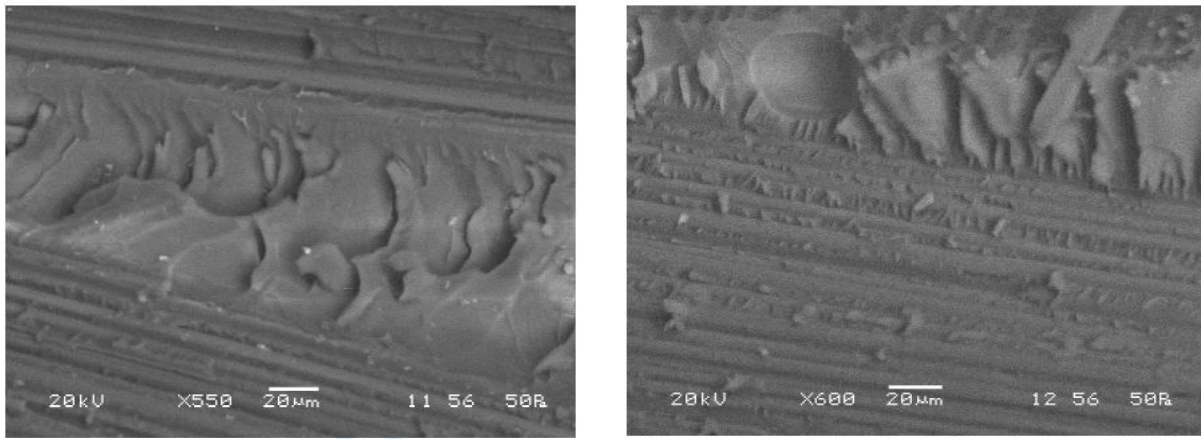

Fig. 4.9 depicts developments of cusp due to shear stress in CFRP

4.1.3 DSC Measurements

The measurement of glass transition temperature (T_g) is very important because it establishes the critical service temperature of the polymer composites and their engineering applications [62]. Polymer composites are used at a temperature below their glass transition temperature. But when they are exposed to thermal conditioning environment, the T_g usually increases. DSC analysis shows an increase in glass transition temperature (T_g) after thermal conditioning for glass/epoxy composites. But for carbon /epoxy systems due to strong adhesion between the fiber and matrix T_g value is more as compared to glass/epoxy systems. But with increase in thermal conditioning time the T_g decreases due to the breakage of secondary bonds. During curing of epoxy two independent networks are created they penetrate each other but are not being covalently bonded.

The mixture of this two independent network is called interpenetrating network (IPN). This delays the transition from glassy to rubbery state as a result the glass transition temperature increases.

Table 4.9 T_g Vs Thermal conditioning time (hrs) for glass/epoxy and carbon/epoxy composites for 2 and 5 hrs

Thermal conditioning time(hrs)	T_g(˚C) for glass/epoxy	T_g(˚C) for carbon/epoxy
0	55.26	80
2	56.66	78
5	58.38	74

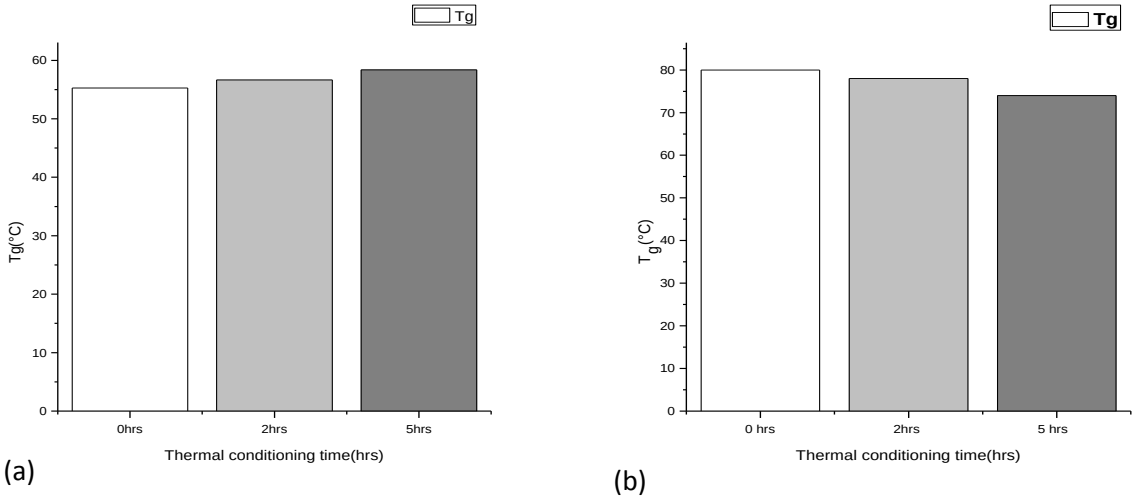

Fig.4.9 T_g Vs Thermal conditioning time for (a) glass/epoxy and (b) carbon/epoxy composites at 50˚C

Due to thermal conditioning the T_g value increases, and it increases with more conditioning time. With increasing T_g the ILSS may increases initially. Hence we are tempted to assume that there is enhancement of mechanical properties.

4.1.4 FTIR Measurements

From the FTIR analysis the band at 2609cm^{-1} in the spectrum of carbon/epoxy composite can't be seen properly in the spectra of the glass/epoxy systems. A new absorbing peak at 2609cm^{-1} is

observed in the spectrum of carbon/epoxy composite shows a bond formation between carbon fiber and epoxy resin. It indicates that epoxy resin has reacted with carbon fiber.

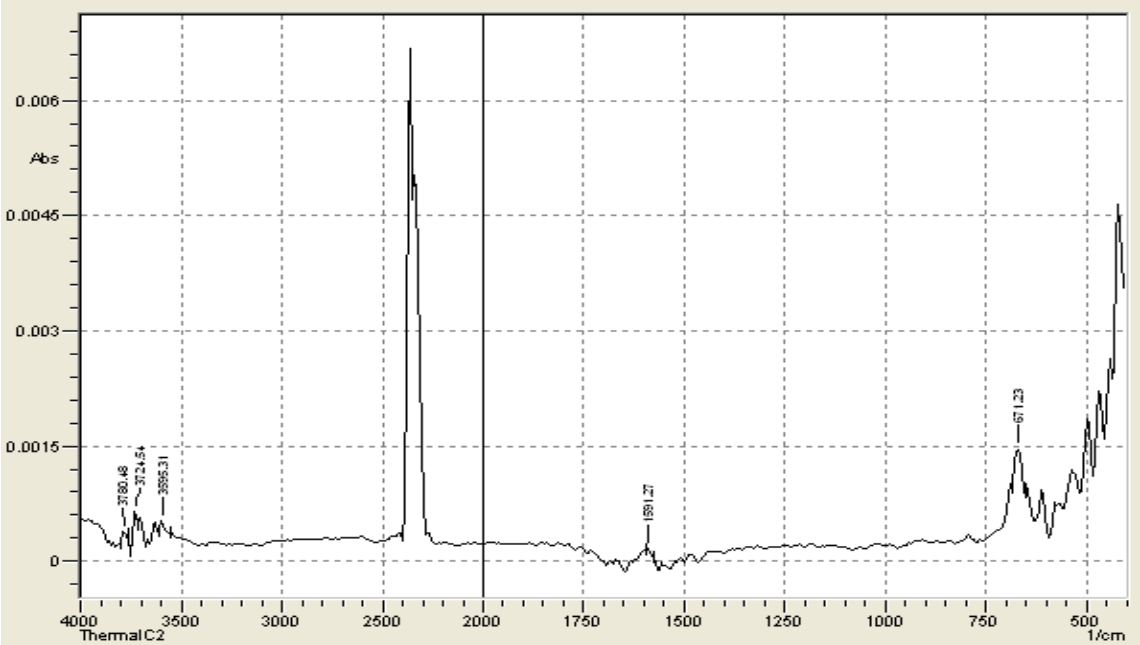

Fig 4.11 represents 2D micrographs taken by FTIR spectrophotometer of untreated glass/epoxy composites

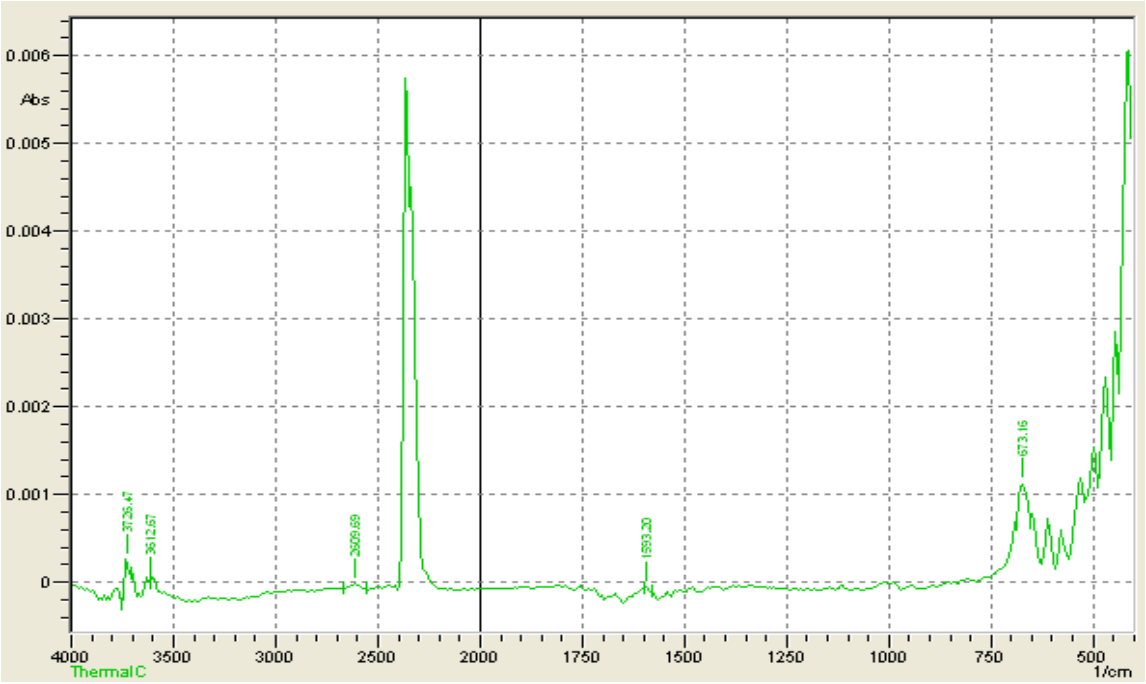

Fig 4.12 represents 2D micrographs taken by FTIR spectrophotometer of untreated glass/epoxy composites

4.1.5 AFM analysis

Composites were subjected to thermal treatment in an oven for 50˚C for 2 hours and 5 hours respectively. AFM surface topography images depicts that the fiber/matrix height difference gradually increased with the increase of thermal treatment time. This increased height difference shows that the matrix shrinks after thermal exposure. The net shrinkage of the resin may be due to the volatile loss and additional cure during thermal treatments. For glass/epoxy composites the vertical distance between the two selected points increased from 2.94µm before treatment to 3.26µm after 5 hours of thermal treatment at 50˚C.

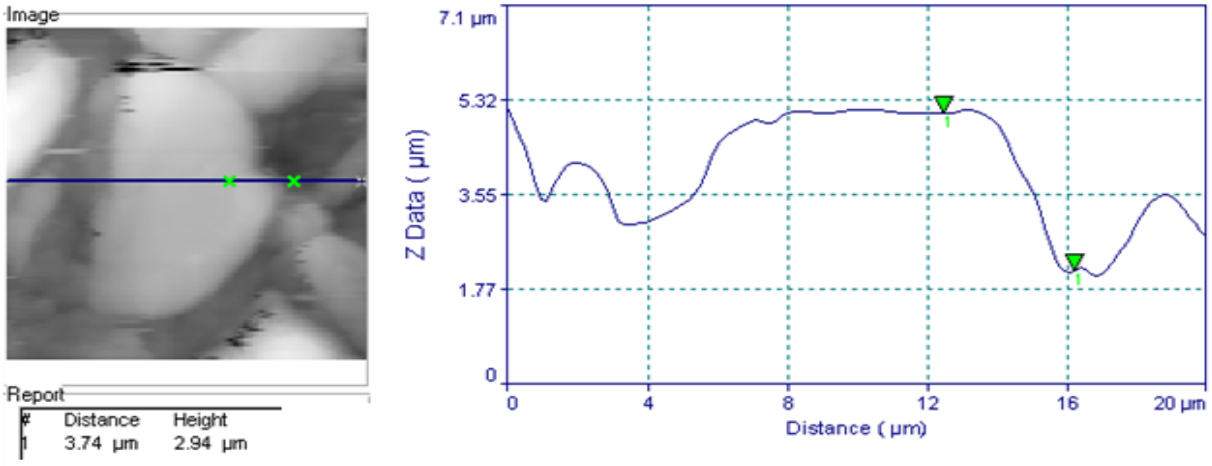

Fig.4.13 Thermal treatment effect on the topography of glass/epoxy composites for 2 hours

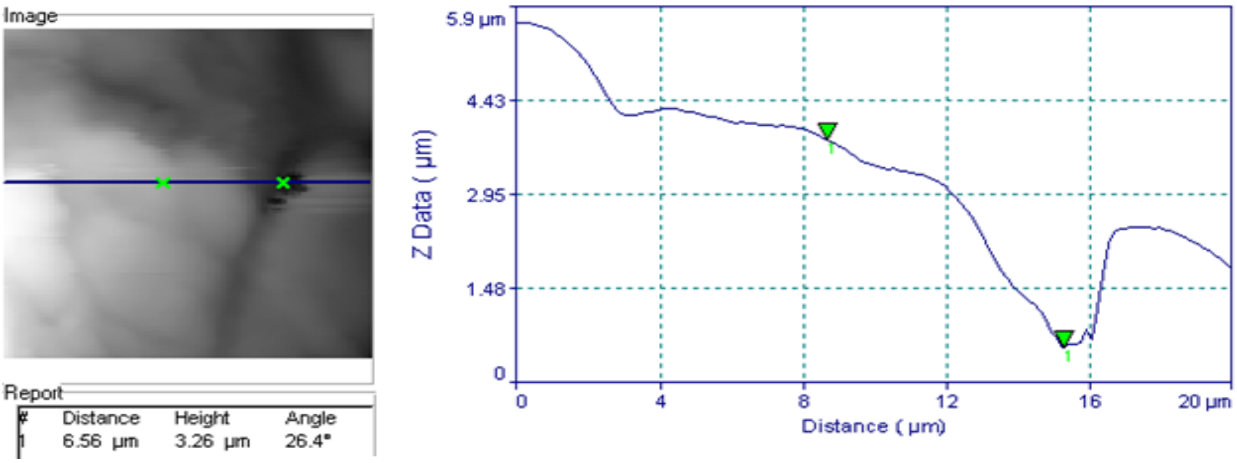

Fig.4.14 Thermal treatment effect on the topography of glass/epoxy composite for 5 hours

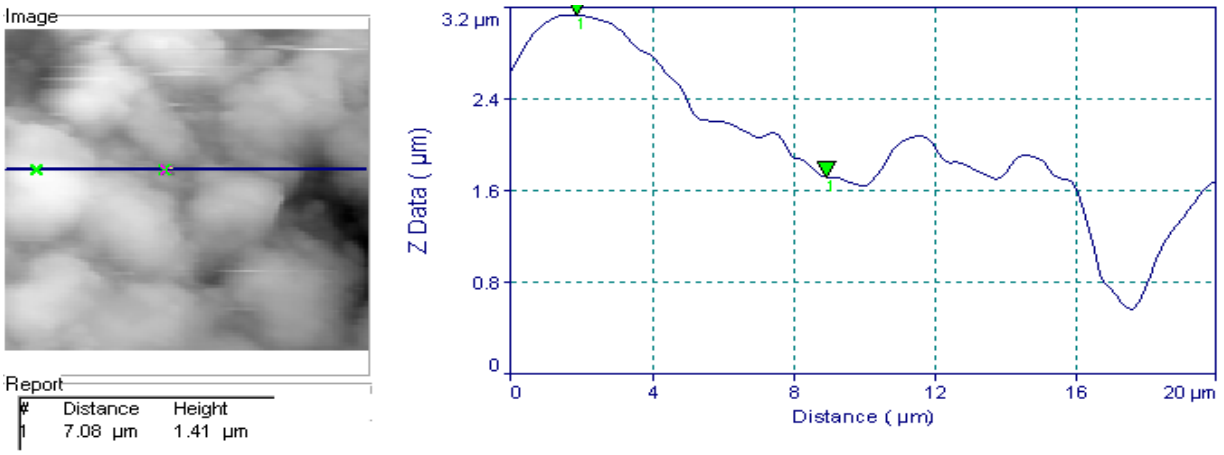

Fig.4.15 Thermal treatment effect on the topography of carbon/epoxy composites for 2 hours

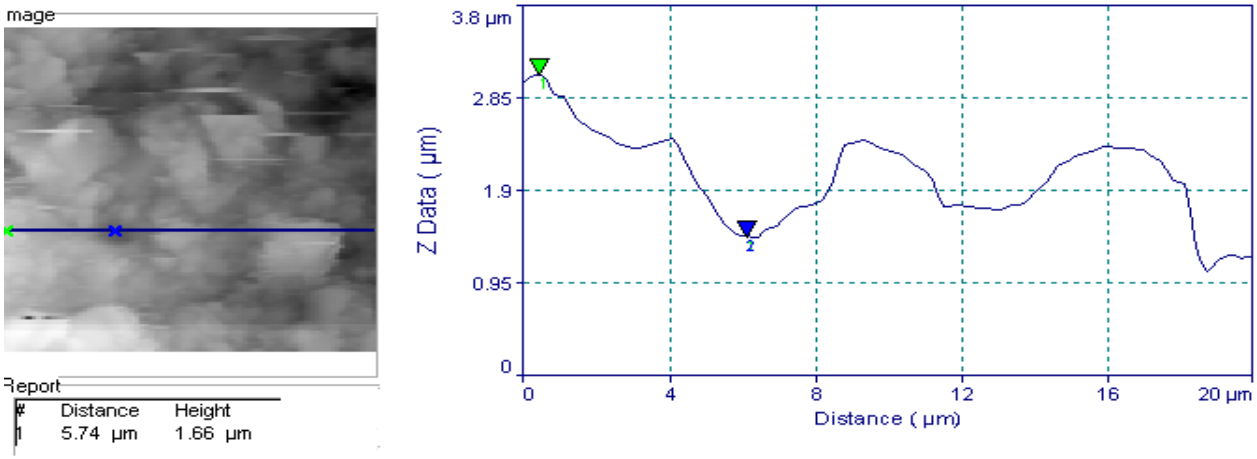

Fig.4.16 Thermal treatment effect on the topography of carbon/epoxy composites for 5 hours

For carbon/epoxy composites the vertical distance between the two selected points increased from 1.41µm before treatment to 1.66µm after 5 hours of thermal treatment at 50˚C.

4.2 Effects of Temperature and Loading Speed on Inter-laminar Strength of FRP Composites

Inter-laminar shear properties are required for analyzing and characterizing the polymer matrix composite structures. These properties of polymer matrix composites under quasi-static loading conditions are well documented but under high strain rate loading are not yet clearly understood. The present investigation is based on the variation of crosshead speed with ILSS for thermal conditioned samples at-, below-, above- ambient and above- the glass transition temperature of glass/epoxy composites

4.2.1 Short Beam Shear Test for glass/epoxy composites

The results obtained from the 3-point bend test reveals that the ILSS at above and below ambient is more as compared to above the glass transition temperature. The glass/epoxy composite losses their rigidity and their strength with increasing temperature, modulus of elasticity and tensile strength in fiber direction decrease rapidly after 60 and 80˚C, respectively and the ILSS decrease nearly linear by increasing temperature [12]. However, high levels of ILSS were realized when the maximum curing temperature was limited to 80°C. Epoxy resin reaches their maximum mechanical properties when they are completely cross-linked or cured. Above T_g they are in a rubbery like state, due to this rubbery state the mechanical properties such as ILSS decreases and it is strain rate sensitive. In the T_g region, the visco-elastic nature of the material is enhanced and the polymer mechanical response becomes highly strain-rate dependent [13].

Table 4.10 Cross head speed Vs. ILSS for glass/epoxy composites at ambient, above ambient and above glass transition temperature

Crosshead speed	ILSS at ambient	ILSS at +50˚C for 2hrs	ILSS at +80˚C for 2hrs
1	18.5	23.8	24.98
10	17.84	17.73	23.82
100	17.26	19.76	25.46
200	18.03	21.78	22.4
500	18.36	22.26	22.66

Table 4.11 Cross head speed Vs. ILSS for glass/epoxy composites at ambient, below ambient and at -80˚C temperature

Crosshead speed	ILSS at ambient	ILSS at -50˚C for 2hrs	ILSS at -80˚C for 2hrs
1	18.5	24.39	19.35
10	17.84	25.84	25.93
100	17.26	25.2	85.53
200	18.03	27.72	84.16
500	18.36	26.38	79.96

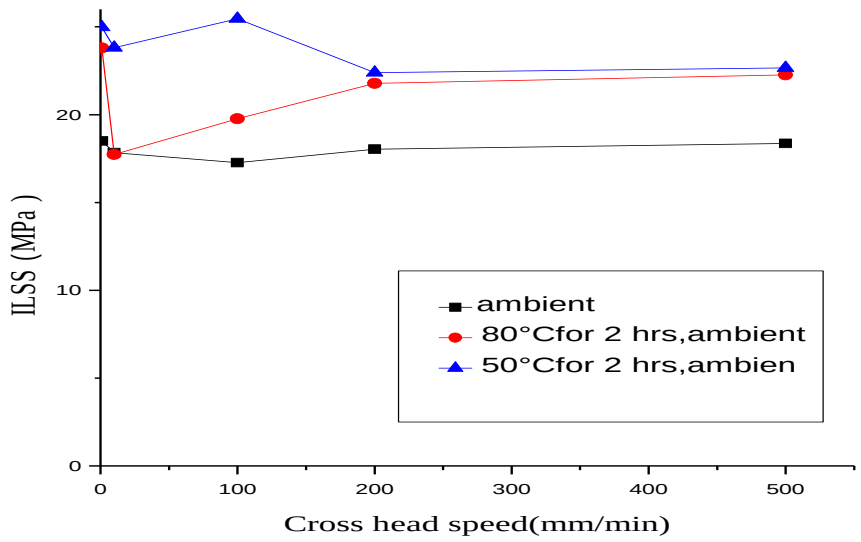

Fig 4.17 Cross head speed Vs. ILSS for glass/epoxy composites at ambient, above ambient and above glass transition temperatures.

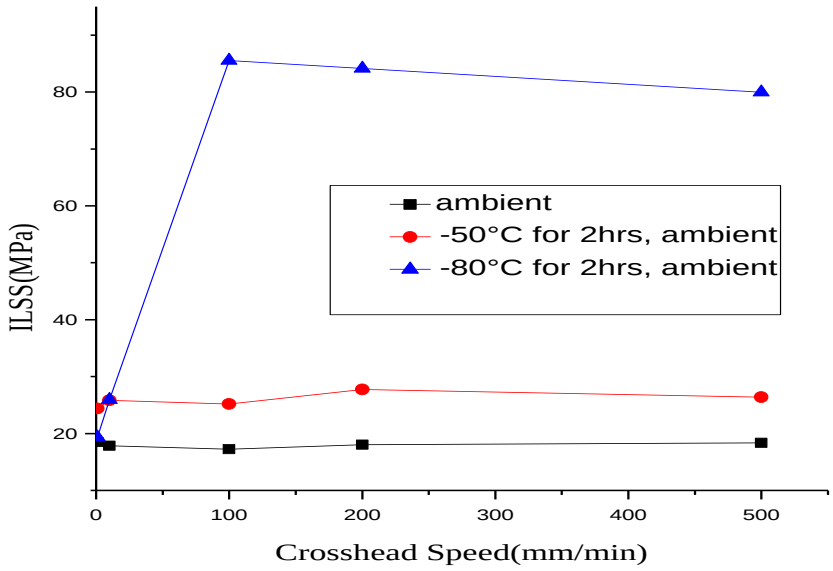

Fig 4.18 Cross head speed Vs. ILSS for glass/epoxy composites at ambient, above ambient and above glass transition temperatures

Larger amount of residual stress develop which is manifested at higher thermal conditioning temperature at 80˚C by differential thermal expansion between the fiber and polymer. The less value of ILSS might be attributed by this residual stresses. This residual stress is quite possibly

decreases the threshold values of crack propagation, it might have resulted less failure stress. At -80°C the ILSS value is higher at higher loading rates; this can be attributed by better adhesion at the interface. The nature of variation appears to be dependent at the conditioning temperature and loading rate.

4.2.2 SEM analysis

Fig 4.19(a) depicts extensive matrix damage by formation of micro and macro crack, failure might have been contributed by matrix failure. Fig.4.19 (b) showing the presence of less fiber/matrix de-bonded area indicates an enhanced adhesion by thermal condition. Higher the ILSS values, strain more there are less fiber pull-out and de-bonded area. The elevated temperature (65°C) causes thermal softening of matrix resin and with increasing load slowly, the damage accumulation process extend and finally it leads to deteriorate [64].

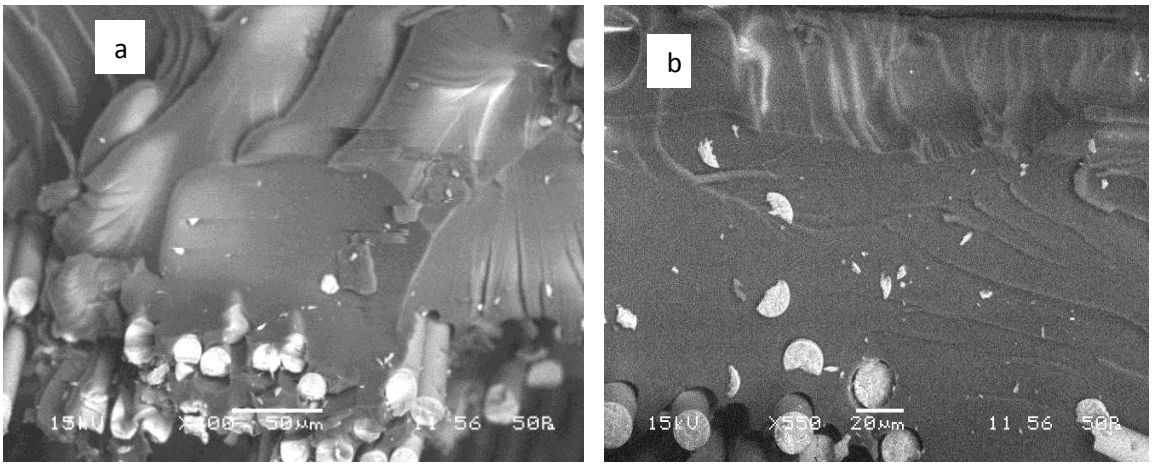

Fig 4.19(a) Scanning electron micrograph of thermal conditioned at 50˚ C and fig.(b) depicts extensive river markings on the matrix at 80°C for glass/epoxy composite

At 80°C temperature more cross linking of the polymer occurs, matrix resin brittleness increases due to rigidity. This rigidity increases strain at the cost of ductility. It was found that, at a temperature of 80°C, the shear strength of the low viscosity epoxy was reduced to about 30% of its value at room temperature. The temperature resistant epoxy behaved well at high temperature, its residual shear strength at 80 °C was 75% of its shear strength at room temperature [65]. SEM micrographs prevails in fig 4.20 that at above ambient (50°C) temperature due to further polymerization adhesion level between fiber and epoxy increases which increases the ILSS.

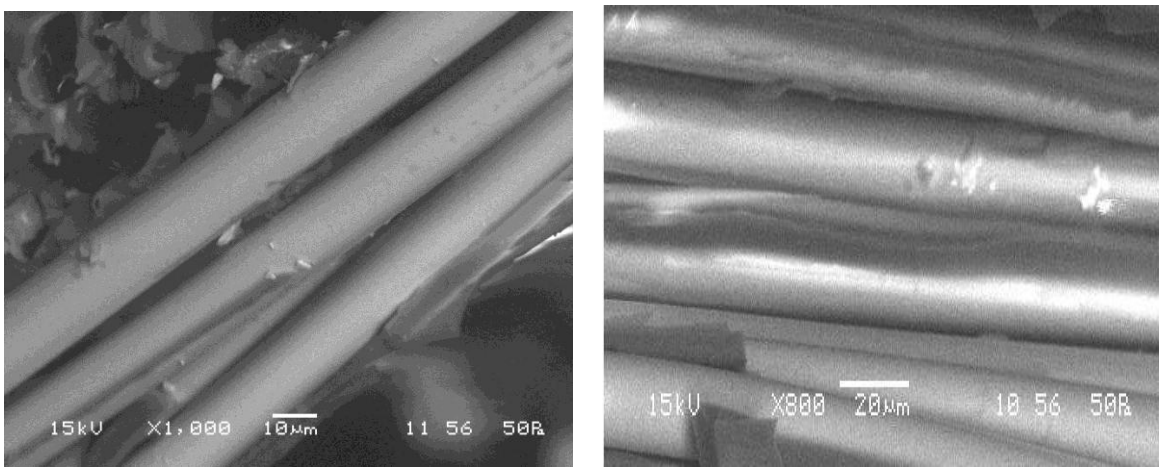

Fig 4.20 SEM micrographs for thermal conditioned samples showing increase the adhesion level between fiber and matrix

Below ambient i.e. at -50°C again the adhesion level increases due to lock and key adhesion mechanism, as a result the ILSS values increases. The localized failure depends on the local microstructure and defect concentration. The microstructure of the polymer matrix is influenced by the conditioning temperature [66]. At -80°C the ILSS values increases with a greater extent due to the generation of more compressive stresses. Better lock and key adhesion mechanism along with low temperature hardening.

CHAPTER 5

CONCLUSIONS

SCOPE FOR FUTURE WORK

Chapter 5

5. Conclusions

1. The Short Beam Shear test results clears that the mechanical properties of epoxy matrix composites depends on the conditions of the tests i.e. the crosshead speed and temperature. The variations of ILSS with crosshead speed are found to be unusual and may be unreported on the open literature. ILSS values increases at above ambient temperature and it may be increased with more conditioning time limited by some optimum value due to post curing. Whereas at below ambient temperature lock and key adhesion mechanism improves ILSS. Glass/epoxy systems are loading rate sensitive up-to 200 mm/min after that they are seemingly less sensitive to loading rate. Whereas carbon/epoxy systems are less sensitive or insensitive to loading rate as compared to glass/epoxy systems.

2. Different failure mechanisms occur at higher crosshead speed due to less relaxation time thus the chances of uniform and gross deformation is reduced. With changing in loading rate from static to dynamic, the failure mechanisms are also changing from fiber fracture to matrix cracking.

3. DSC results predicts that the T_g increases with thermal conditioning time for glass/epoxy where as it may decreases for carbon/epoxy due to strong adhesion.

4. FTIR spectroscopy analysis showing new absorption spectra at 2609 cm^{-1} for carbon/epoxy composites.

5. AFM surface topography reveals that for glass/epoxy composites the vertical distance between the two selected points increased from 2.94μm before treatment to 3.26μm after 5 hours of thermal treatment at 50˚C and for carbon/epoxy this distance increased from 1.41μm to 1.66μm.

SCOPE FOR FUTURE WORK

In summary the present piece of work leaves a wide scope for future investigators to explore many other aspects of loading rate sensitivity of thermal conditioned FRP composites at different temperatures. The complex failure mechanisms of glass/epoxy and carbon/epoxy composites require more experimentation for a better characterization of these materials. Implications of thermal conditioning most often lead an improved adhesion of the interface (at above- ambient) and/or increased crack density (at below- ambient) temperatures. These changes might lead further complications in accessing the loading rate sensitivity which itself as contradictory as on today.

References

1. Kelly A, Zweben C., Comprehensive Composite Materials. Oxford U.K, Elsevier Science Publication, 2000

2. Bunsell A R and Renard J., Fundamentals of fiber reinforced composite materials. London, Institute of Physics, 2005

3. Kaw A K., Mechanics of Composite Materials. University of South Florida, Tampa, USA, Taylor & Francis, 2006

4. Jang B Z., Advanced Polymer Composites: Principle and Applications. ASM International, Materials Park, OH, 1994

5. Callister W D., Materials Science and Engineering: An Introduction. Asia, John Wiley and Sons, 2001

6. Aggarwal B D, Broutman L J., Analysis and performance of Fiber Composites. Canada, Wiley Inter science, 1990

7. Hull D, Clyne T W., An Introduction to Composite Materials. Cambridge, U.K, Cambridge University Press, 1996

8. Zulkifli R. Surface Fracture Analysis of Glass Fibre Reinforced Epoxy Composites Treated with Different Type of Coupling Agent European Journal of Scientific Research, 29 (1) (2009):pp. 55-65

9. Kim K, Mai Y W., Engineered Interfaces in Fiber Reinforced Composites. Kidlington, Oxford U.K, Elsevier Publication, 1998

10. Lee S M., Handbook of Composite Materials. New York: VCH Publishers, 1993

11. Kanchanomai C, Rattananon S, Soni M. Effects of loading rate on fracture behavior and mechanism of thermoset epoxy resin, Polymer Testing, 24(2005) :pp.886- 892

12. Jacob G C, Starbuck J M, Fellers J F, Simunovic S and Boeman R G. Strain Rate Effects on the Mechanical Properties of Polymer Composite Materials, Journal of Applied Polymer Science, 94 (2004):pp.296- 301.

13. Hamouda A M S, Hashmi M S J. Testing of composite materials at high rates of strain: advances and challenges, Materials Processing Technology, 77(1998):pp. 327-336

14. Tanoglu M, McKnight S H, Palmese G R and Gillespie J W. A new technique to characterize the fiber/matrix interphase properties under high strain rates, Composites Part A, 31 (2000):pp.1127-1138.

15. Barre S, Chotard T and Benzeggagh M L. Comparative study of strain rate effects on mechanical properties of glass fibre reinforced thermoset matrix composites, Composites Part A 27A(1996):pp.1169-1181

16. Okoli O I. The effects of strain rate and failure modes on the failure energy of fibre reinforced composites, Journal of Composite structure, 54(2001):pp.299-303

17. Saniee F F, Majzoobi G H, Bahrami M. An experimental study on the behavior of glass–epoxy composite at low strain rates, Journal of Materials Processing Technology, 162 (2005): pp. 39–45.

18. Harding, J. & Welsh, L. M. A tensile testing technique for fibre-reinforced composite at impact rates of strain, Journal of material Science, 18 (1983):pp. 1810-26.

19. Ochola R O, Marcus K, Nurick G N and Franz T. Mechanical behaviour of glass and carbon fibre reinforced composites at varying strain rates, Composite Structures, 63(2004) :pp.455-467

20. Naruse T, Hattori T, Miura H, Takahashi K. Evaluation of thermal degradation of unidirectional CFRP rings, Composite Structures 2001;52: 533

21. Kaiser T. Highly cross-linked polymers, Progress in Polymer Science, 14(1989):pp.373-450

22. Ray BC. Thermal shock on interfacial adhesion of thermally conditioned glass fiber/epoxy composites rates, Materials Letters, 58(2004):pp.2175-2177

23. Naik N K, Yernamma P, Thoram N M, Gadipatri R, Kavala.V R. High strain rate tensile behavior of woven fabric E-glass/epoxy composite, Polymer Testing 29(2010):pp.14-22

24. Hartwig G., Polymer properties at room and cryogenic temperatures. New Work, Plenum Press, 1994

25. Abdel-Magid B, Ziaee S, Gass K, Schneider M. The combined effects of load, moisture and temperature on the properties of E-glass/epoxy composites, Composite Structures,71(2005): pp. 320-326.

26. Dieter G E., Mechanical Metallurgy. UK, McGraw Hill, 1988

27. Hahn H T and Pagano N J. Curing Stresses in Composite Laminates, Composite Materials, 9 (1975):pp.91-106

28. Okoli, O I, Smith G F. Aspects of the Tensile Response of Random Continuous Glass/Epoxy Composites, Journal of Reinfoced Plastics and Composites, 18 (1999):pp.606-613

29. Okoli O I., Smith G F. Failure modes of fiber reinforced composites: The effect of strain rate and fiber content, Journal of Materials Science, 33 (1998):pp. 5415 – 5422

30. Shokrieh M M, Omidi M J. Tension behavior of unidirectional glass/epoxy composites under different strain rates, Composite Structures, 88 (2009):pp. 595–601

31. Ray B C. Effect of crosshead velocity and sub-zero temperature on mechanical behavior of hygrothermally conditioned glass fiber reinforced epoxy composites, Material Science and Engineering A 397(1–2) (2004): pp.39-44

32. Hardin J and Li Y L. Determination of interlaminar shear strength for glass/epoxy and carbon/epoxy laminates at impact rates of strain , Composites Science and Technology, 45 (1992):pp. 161-171

33. Gilat A, Goldberg R K, Roberts G D. Experimental study of strain-rate-dependent behavior of carbon/epoxy composite , Composites Science and Technology, 62 (2002):pp. 1469–1476

34. Hartwig G and Knaak S. Fibre-epoxy composites at low temperatures, Cryogenics, 24(1984):pp.639-647

35. Ganczakowski H L and Beaumont P W R. The Behaviour of Kevlar Fibre-Epoxy Laminates under Static and Fatigue Loadings. Part I-Experimental, Composites Science and Technology, 36 (1989):pp. 299-319

36. Hertzberg R W. Deformation and Fracture Mechanics of Engineering Materials, John Wiley & Sons, 1996

37. Purslow D. Matrix fractography of fibre reinforced epoxy composites, Composites, 17 (4) (1986):pp.289- 303

38. Kellogg K G, Patil R, Kallmeyer A R, Dutta P K. Effect of Load Rate on Notch Toughness of Glass FRP Subjected to Moisture and Low Temperature , International Journal of Offshore and Polar Engineering, 15(1), (2005):pp. 54–61

39. Ray B C. Adhesion of glass/epoxy composites influenced by thermal and cryogenic environments, Journal of Applied Polymer Science, 102(2) (2006): pp.1943-1949.

40. Yano O and Yamaoka H. Cryogenic Properties of Polymers, Progress in Polymer Science, 20(1995):pp.585-613

41. Naruse T, Hattori T, Miura H, Takahashi K. Evaluation of thermal degradation of unidirectional CFRP rings, Composite Structures, 52 (2001):pp. 533-538.

42. Colin X, Verdu J. Strategy for studying thermal oxidation of organic matrix composites, Composite Science and Technology, 65(3-4) (2005):pp.411-419

43. Seyler R J. Assignment of the Glass Transition, Philadelphia, ASTM STP 1249, 1994

44. Wang.Y , Thomas H. Hahn. AFM characterization of the interfacial properties of carbon fiber reinforced polymer composites subjected to hygrothermal treatments ,Composites Science and Technology, 67 (2007):pp. 92-101

45. Aktas M, Karakuzu R. Determination of mechanical properties of glass-epoxy composites in high temperatures, Polymer Composites, 30 (2009) :pp.1437-1441

46. Morioka K, Tomita Y, Takigawa K. High-temperature fracture properties of CFRP composite for aerospace applications, Materials Science and Engineering A, 319–321 (2001):pp. 675–678

47. Barjasteh E, Bosze E J, Tsai YI, Nutt S R. Thermal aging of fiberglass/carbon-fiber hybrid composites, Composites Part A, 40 (2009):pp. 2038- 2045

48. Salin I, Seferis J C. Anisotropic degradation of polymeric composites: from neat resin to composite, Polymer Composites, 13(1996):pp. 430

49. Borje A, Aders S and Lars B. Micro- and meso- level residual stresses in glass/vinyl-ester composite, Composite Science and Technology, 60(2000):pp.2011-2028

50. Timmerman J F, Tillman M S, Matthew S, Hayes, Brian S, Seferis J C. Matrix and fiber influences on the cryogenic micro cracking of carbon fiber/epoxy composites, Composites Part A: Applied Science and Manufacturing,33(3) (2002): pp.323-329

51. Kaelble D H, Dynes P J, L Maus. Hydrothermal Aging of Composite Materials Part 1:Interfacial Aspects , Adhesion 8(1976):pp.121-144

52. Marom G and Broutman L J. Moisture penetration into composites under external stress, Polymer Composites, 2(3) (1981):pp. 132–136

53. Mijovic J and Lin K F. The effect of hygrothermal fatigue on physical/mechanical properties and morphology of neat epoxy resin and graphite/epoxy composite, Journal of Applied Polymer Science, 30(1985):pp. 2527-2549.

54. Ray B C. Temperature effect during humid ageing on interfaces of glass and carbon fiber reinforced epoxy composites, Journal of Colloid and Interface Science,298 (2006): pp. 111-117.

55. ASTM D 2344, Test method for apparent interlaminar shear strength of parallel fiber composites by Short Beam Method, American Society for Testing and Materials, West Conshohocken, PA, 1995

56. Whitney J M and Browning C E. On Short Beam Shear Tests for Composite Material, Experimental Mechanics, 25 (1985):pp.294-300

57. Brooks C R and Choudhury A., Metallurgical Failure Analysis. New York, McGraw-Hill, 1992

58. Gonzalez-Benito J. The nature of structure gradient in epoxy curing at a glass fiber/epoxy matrix interface using FTIR imaging, Journal of Colloid Interface Science,267 (2003): pp.326-332.

59. Kalsi P S., Spectroscopy of Organic Compounds. New Delhi, New Age International, 2005

60. Ray B C. Thermal shock on interfacial adhesion of thermally conditioned glass fiber/epoxy composites, Materials Letters, 58 (2004): pp. 2175-2177.

61. Surendra Kumar M, Sharma N and Ray B C. Microstructural and Mechanical Aspects of Carbon/Epoxy Composites at Liquid Nitrogen Temperature, Journal of Reinforced Plastics and Composites, 28(2009*)*, pp. 2013-2023

62. Zhou J, Lucas J P. Hygrothermal effects of epoxy resin. Part II: variations of glass transition temperature, Polymer, 40,(1999): pp. 5513-5522

63. Detassis M, Pegoretti A and Migliaresi C. Effect of temperature and strain rate on interfacial shear stress transfer in carbon/epoxy model composites Composite Science and Technology, 53 (1995):pp. 39-46

64. Xiaoping H, Shenliang H, Liang Y. A study on dynamic fracture toughness of composite laminates at different temperatures, Composites Science and Technology, 63 (2003):pp.155–159

65. Saafi M. Effect of fire on FRP reinforced concrete members, Composite Structures, 58 (2002):pp.11–20

66. Ray B C. Loading Rate effects on Mechanical Properties of Polymer Composites at Ultralow Temperatures, Journal of Applied Polymer Science, 100 (2006):pp.2289-2292

APPENDIX: SHORT BEAM SHEAR TEST RESULTS

GLASS/EPOXY AT +50˚C FOR 2HRS

Specimen no.	Width(mm)	Thickness(mm)	Crosshead speed(mm/min)	Load at yield(KN)	Strain at yield(mm/mm)
1	5.65	4.88	1	0.4977	.0071
2	5.87	4.67	1	0.5705	0.0190
3	5.87	4.88	1	0.3346	0.0118
4	5.85	4.72	10	0.7380	0.0265
5	5.70	4.86	10	0.5397	0.0289
6	6.03	4.87	10	0.6074	0.0284
7	5.87	4.9	100	0.4853	0.0706
8	5.81	4.61	100	0.5143	0.0127
9	5.60	4.7	100	0.4803	0.0129
10	5.73	4.85	200	0.6540	0.0333
11	5.91	4.87	200	0.7687	0.0267
12	5.81	4.9	200	0.4562	0.0269
13	5.96	4.8	500	0.7740	0.0380
14	5.92	4.66	500	0.6538	0.0325
15	5.92	4.64	500	0.5987	0.0221

GLASS/EPOXY AT +50˚C FOR 5HRS

Specimen no.	Width(mm)	Thickness(mm)	Crosshead speed(mm/min)	Load at yield(KN)	Strain at yield(mm/mm)
1	6.39	5.23	1	1.023	0.0349
2	6.28	5.25	1	1.169	0.0369
3	6.14	5.25	1	1.016	0.0385
4	6.21	5.07	10	1.110	0.0367
5	6.20	5.00	10	1.036	0.0309
6	6.08	4.86	10	1.026	0.0350
7	6.14	4.86	100	0.9951	0.0066
8	6.08	5.36	100	1.028	0.0082
9	6.18	5.09	100	1.131	0.0086
10	6.29	5.13	200	1.164	0.0159
11	6.13	5.24	200	1.199	0.0199
12	6.26	5.26	200	1.189	0.0199
13	6.28	5.05	500	1.123	0.0601
14	6.24	5.22	500	1.146	0.0413
15	6.19	5.11	500	1.106	0.0442

GLASS/EPOXY AT −50˚C FOR 2HRS

Specimen no.	Width(mm)	Thickness(mm)	Crosshead speed(mm/min)	Load at yield(KN)	Strain at yield(mm/mm)
1	6.08	4.92	1	0.6512	0.0214
2	6.08	5.00	1	0.05259	0.0199
3	6.14	5.1	1	0.07363	0.0237
4	6.02	5.1	10	0.8338	0.1026
5	6.14	4.85	10	0.7787	0.0251
6	6.04	4.94	10	0.8413	0.0272
7	5.97	4.98	100	0.7941	0.0140
8	6.15	5.04	100	0.7377	0.0118
9	6.04	4.9	100	0.7477	0.0119
10	6.12	4.89	200	0.7702	0.0274
11	6.16	4.76	200	0.5785	0.0235
12	6.00	4.97	200	0.8199	0.0151
13	6.12	5.11	500	0.8241	0.0318
14	6.11	4.98	500	0.7715	0.0533
15	5.97	4.86	500	0.6764	0.0543

GLASS/EPOXY AT −50˚C FOR 5HRS

Specimen no.	Width(mm)	Thickness(mm)	Crosshead speed(mm/min)	Load at yield(KN)	Strain at yield(mm/mm)
1	6.14	4.92	1	0.92853	0.0252
2	6.07	4.81	1	0.8732	0.0324
3	6.14	4.86	1	0.9562	0.0333
4	6.05	4.83	10	1.0540	0.0415
5	6.18	4.81	10	1.185	0.0377
6	6.05	4.91	10	0.9742	0.0279
7	6.01	5.04	100	1.0910	0.010
8	6.04	5.12	100	1.116	0.0097
9	6.07	4.96	100	0.9860	0.0081
10	6.11	4.59	200	1.1720	0.0205
11	6.07	5.02	200	0.9838	0.0142
12	6.09	4.90	200	1.0540	0.0152
13	6.00	4.75	500	1.011	0.0434
14	5.97	4.91	500	0.9905	0.0423
15	6.15	4.83	500	0.9980	0.0362

CARBON/EPOXY AT AMBIENT

Specimen no.	Width(mm)	Thickness(mm)	Crosshead speed(mm/min)	Load at yield(KN)	Strain at yield(mm/mm)
1	6.6	8.15	1	2.668	0.0312
2	6.32	7.52	1	2.759	0.0311
3	6.48	7.41	1	2.779	0.0271
4	6.36	7.71	10	2.474	0.0243
5	6.45	7.76	10	2.363	0.0229
6	6.74	8.71	10	2.744	0.0252
7	6.71	7.98	100	1.479	0.0219
8	6.68	8.36	100	1.897	0.0287
9	6.37	7.75	100	1.744	0.0213
10	6.71	7.77	200	1.585	0.0427
11	6.45	7.45	200	1.610	0.0409
12	6.41	8.22	200	1.891	0.0451
13	6.8	8.11	500	1.763	0.1114
14	6.0	8.30	500	1.508	0.106
15	6.5	7.67	500	1.528	0.079

CARBON/EPOXY AT +50˚C FOR 2HRS

Specimen no.	Width(mm)	Thickness(mm)	Crosshead speed(mm/min)	Load at yield(KN)	Strain at yield(mm/mm)
1	6.36	7.7	1	2.771	0.0408
2	6.51	8.2	1	2.571	0.037
3	7.04	8.28	1	2.130	0.059
4	6.25	7.54	10	2.024	0.0378
5	6.5	8.03	10	2.245	0.0408
6	6.53	7.34	10	2.054	0.0292
7	6.28	8.24	100	1.508	0.0283
8	6.78	7.64	100	2.134	0.0210
9	6.92	8.15	100	2.365	0.0224
10	6.32	7.8	200	2.165	0.0428
11	6.44	7.87	200	2.430	0.0432
12	6.5	7.81	200	2.145	0.0429
13	6.36	7.95	500	2.326	0.01092
14	6.5	7.84	500	2.365	0.1077
15	6.21	7.94	500	2.069	0.1090

CARBON/EPOXY AT +50˚C FOR 5HRS

Specimen no.	Width(mm)	Thickness(mm)	Crosshead speed(mm/min)	Load at yield(KN)	Strain at yield(mm/mm)
1	6.85	8.51	1	1.109	0.0002
2	7.69	8.50	1	3.813	0.0377
3	7.80	8.12	1	2.352	0.0323
4	7.53	6.95	10	2.648	0.0310
5	7.48	6.68	10	2.398	0.0319
6	6.85	7.57	10	2.198	0.0280
7	7.35	6.86	100	1.472	0.0082
8	7.33	7.48	100	1.658	0.0099
9	7.33	7.22	100	1.409	0.0055
10	7.37	7.6	200	2.461	0.0329
11	7.46	6.93	200	2.440	0.0266
12	7.63	7.49	200	2.468	0.0189
13	7.76	7.56	500	2.898	0.0536
14	7.47	6.8	500	2.352	0.0518
15	8.22	8.45	500	2.351	0.0562

CARBON/EPOXY AT −50˚C FOR 2HRS

Specimen no.	Width(mm)	Thickness(mm)	Crosshead speed(mm/min)	Load at yield(KN)	Strain at yield(mm/mm)
1	6.99	7.88	1	2.618	0.0294
2	6.33	8.30	1	2.808	0.0322
3	6.20	7.79	1	2.509	0.0278
4	6.96	7.72	10	2.357	0.0200
5	6.28	8.23	10	2.250	0.0215
6	6.42	7.77	10	2.149	0.0351
7	6.92	7.98	100	2.126	0.0146
8	6.41	7.90	100	1.95	0.0165
9	6.39	7.80	100	2.048	0.0161
10	6.81	8.03	200	1.741	0.0167
11	6.42	8.30	200	1.585	0.0155
12	6.34	8.05	200	1.525	0.0207
13	6.85	7.85	500	2.046	0.0306
14	6.44	8.18	500	1.998	0.0295
15	6.50	8.7	500	2.222	0.0318

GLASS/EPOXY AT 80˚C FOR 2HRS TESTING AT AMBIENT

Specimen no.	Width(mm)	Thickness(mm)	Crosshead speed(mm/min)	Load at yield(KN)	Strain at yield(mm/mm)
1	7.66	8.56	1	3.493	0.0331
2	7.68	6.83	1	2.983	0.0337
3	7.27	7.01	1	2.842	0.0326
4	7.62	8.52	10	2.496	0.0328
5	7.34	7.00	10	3.160	0.0287
6	7.34	7.00	10	2.753	0.0282
7	7.9	8.56	100	2.198	0.0138
8	7.29	7.70	100	2.753	0.0071
9	7.72	6.95	100	1.987	0.0048
10	7.19	8.62	200	1.289	0.0169
11	7.37	6.77	200	1.695	0.0148
12	7.24	7.11	200	1.985	0.0129
13	7.10	7.58	500	1.582	0.0418
14	7.22	7.57	500	1.985	0.0456
15	7.31	6.7	500	2.234	0.0642

GLASS/EPOXY AT -80˚C 2HRS FOR 2HRS TESTING AT AMBIENT

Specimen no.	Width(mm)	Thickness(mm)	Crosshead speed(mm/min)	Load at yield(KN)	Strain at yield(mm/mm)
1		8.56	1	3.493	0.0331
2	7.68	6.83	1	2.983	0.0337
3	7.27	7.01	1	2.842	0.0326
4	7.62	8.52	10	2.496	0.0328
5	7.34	7.00	10	3.160	0.0287
6	7.34	7.00	10	2.753	0.0282
7	7.9	8.56	100	2.198	0.0138
8	7.29	7.70	100	2.753	0.0071
9	7.72	6.95	100	1.987	0.0048
10	7.19	8.62	200	1.289	0.0169
11	7.37	6.77	200	1.695	0.0148
12	7.24	7.11	200	1.985	0.0129
13	7.10	7.58	500	1.582	0.0418
14	7.22	7.57	500	1.985	0.0456
15	7.31	6.7	500	2.234	0.0642

PERSONAL PROFILE

Renu prava Dalai
M.Tech.
Department of Metallurgical and Materials Engineering
National Institute of Technology Rourkela,
Rourkela-769008,India
Telephone no.-09861926292
Email.id-dalai.renu@gmail.com

Professional Qualifications:

Bachelor Degree in metallurgical Engineering (B.Tech) from B.P.U.T, Rourkela, India
Master Degree in Metallurgical and Materials Engineering (M.Tech) from National Institute of Technology Rourkela, India.

Experience

2 years and 6 months experience as a faculty in the Department of Metallurgical and Materials Engineering at I.G.I.T Sarang(Orissa),India.

Reasearch interest is on the loading rate sensitivity of FRP composites and its environmental implications.

LIST OF PUBLICATIONS

1) Dalai.R.P, Ray.B.C, An assessment of mechanical behavior of fibrous polymeric composites under different loading speeds at above- and sub- ambient temperatures, Journal of Materials Letters, Submitted.

2) Dalai.R.P, Ray.B.C,A review on effect of loading rate and temperature on FRP composites: An emphasis on microstructural implication, Journal of Composite Materials, Submitted.

3)Dalai.R.P, B.B.Verma and Ray.B.C, Effects of above- and sub- ambient temperature conditioning on failure and fracture modes of advanced fibrous polymeric composites, 3rd National Symposium for Materials Research Scholars and Workshop on Advanced Characterization Technique(MR10), Indian Institute of Technology Bombay.

4) Dalai.R.P, Ray.B.C, Loading rate sensitivity of fibrous composites, International Conference on Recent Trends in Materials and Characterization (RETMAC 2010), National Institute of Technology, Suratkal, Karnataka.

5) Dalai.R.P, Ray.B.C, Effects of Temperature and loading speed on interlaminar strength of FRP composite, 9th International Conference on Durability of Composite Systems, University of Patras, Greece.